AD_____

Award Number: DAMD17-96-1-6289

TITLE: High Temperature Superconductor RF Probes for Breast Cancer Research

PRINCIPAL INVESTIGATOR: Paul C. Wang, Ph.D.

CONTRACTING ORGANIZATION: Howard University
Washington, DC 20059

REPORT DATE: October 2001

TYPE OF REPORT: Final

PREPARED FOR: U.S. Army Medical Research and Materiel Command
Fort Detrick, Maryland 21702-5012

DISTRIBUTION STATEMENT: Approved for Public Release;
Distribution Unlimited

REPORT DOCUMENTATION PAGE

Form Approved
OMB No. 074-0188

1. AGENCY USE ONLY (Leave blank)	2. REPORT DATE	3. REPORT TYPE AND DATES COVERED
	October 2001	Final (20 Sep 96 - 19 Sep 01)

4. TITLE AND SUBTITLE
High Temperature Superconductor RF Probes for Breast Cancer Research

5. FUNDING NUMBERS
DAMD17-96-1-6289

6. AUTHOR(S)
Paul C. Wang, Ph.D.

7. PERFORMING ORGANIZATION NAME(S) AND ADDRESS(ES)
Howard University
Washington, DC 20059

E-Mail: pwang@howard.edu

8. PERFORMING ORGANIZATION REPORT NUMBER

9. SPONSORING / MONITORING AGENCY NAME(S) AND ADDRESS(ES)
U.S. Army Medical Research and Materiel Command
Fort Detrick, Maryland 21702-5012

10. SPONSORING / MONITORING AGENCY REPORT NUMBER

11. SUPPLEMENTARY NOTES
Report contains color

12a. DISTRIBUTION / AVAILABILITY STATEMENT
Approved for Public Release; Distribution Unlimited

12b. DISTRIBUTION CODE

13. ABSTRACT *(Maximum 200 Words)*

Nuclear magnetic resonance imaging and spectroscopy techniques have been used to study the breast cancer cells and tumor grown on animal. The goal of this study is to gain knowledge, which could be useful to improve the specificity of diagnosis and staging of breast cancer in clinic. Intrinsically, NMR techniques have weak signals, which limit the ultimate spatial resolution in image and sensitivity in spectrum. A high temperature superconductor RF probe has been constructed, which has a Q value 650, to improve NMR sensitivity. An improved cell perfusion system was made to continuously run spectroscopy study longer than 8 days. Many phosphorus metabolites of MCF7 breast cancer cells have been identified. There is a subtle difference between MCF7/WT and MCF7/ADR cells. Glycerophosphocholine is lower than phosphocholine for the MCF7/ADR cells. 2 μM Doxorubicin dramatically affected MCF7/WT cells but not MCF7/ADR cells. T1 relaxation times of the phosphorus metabolites are measured. The NMR spectrum shows significant lower PC and ATP and higher Pi signals in tumor than the muscle. High-resolution imaging technique with injection of contrast agent shows a significant non-uniform image enhancement throughout the tumor. Small blood vessels can be identified at peripherals but not at the core of tumor.

14. SUBJECT TERMS
Breast Cancer, magnetic resonance spectroscopy (MRS), magnetic resonance imaging (MRI), cancer cell metabolism, high temperature superconductor

15. NUMBER OF PAGES
38

16. PRICE CODE

17. SECURITY CLASSIFICATION OF REPORT	18. SECURITY CLASSIFICATION OF THIS PAGE	19. SECURITY CLASSIFICATION OF ABSTRACT	20. LIMITATION OF ABSTRACT
Unclassified	Unclassified	Unclassified	Unlimited

Table of Contents

V. Introduction

Conventional mammography has been shown to play an important role in detection and staging of breast cancer in older women. For younger women who frequently have radiodense breast tissue or women with silicon implants, rendering breast cancer diagnosis with conventional mammography is problematic. When mammographic findings and clinical findings concur regarding the possibility of a lesion being malignant, usually a fine-needle aspiration biopsy will be performed for definitive diagnosis. The false positive rate is high; only 20-30% of lesions suspicious for cancer at mammogram are actually positive for cancer at biopsy (1). In general, mammography is limited to detect a tumor several millimeters or larger in size. Because of difficulty with early detection, clinicians are sometimes limited to treat larger size cancers, which in many cases have already metastasized. Accurate definition of tumor size, number, and margins is highly critical in the clinical determination of conservation treatment versus mastectomy. A role exists for an imaging method that can improve sensitivity for detection of small lesion and to improve the specificity for better staging of the disease. To provide the best chance of overall survival, breast cancers need to be accurately staged for systemic treatment and optimal conservation surgery. Traditionally, the gold standards for such assessments are clinicopathological staging and histopathological typing and grading of malignancy. In the classical histopathological approach problems exist inherently, predominantly, the accuracy of the initial biopsy procedure and the variable skills applied to its histological assessment (2). Development of a new modality to remove sampling errors, improve specificity and produce a grading of tissues that relates to establish biological criteria would be very useful.

Over the last few years, magnetic resonance imaging (MRI) and spectroscopy (MRS) have emerged as one of the most promising clinical tools to fill the gap between clinical needs and information obtained by conventional breast imaging and pathological methods (3-13). Preliminary results indicate that MRI may be more sensitive than conventional x-ray mammography in detecting small lesions (14-16). Cancers have typical metabolic characteristics in ^{31}P and ^{1}H MRS including high levels of phospholipid metabolites and a cellular pH more alkaline than normal (17-24). Although these alone are not unique for cancer they are very useful diagnostic information in appropriate clinical settings. MRS is capable of distinguishing benign and malignant lesions in a particular anatomical site and to be a specific diagnostic discriminant in a particular situation. It has been demonstrated to be useful to improve the specificity of the MR imaging of breast (25-36). Some metabolic characteristics appear to be prognostic indices and correlate well with the response of treatment. The improvement of specificity will reduce the number of biopsies performed to confirm false-positive mammographic findings and more effectively assess the results of treatment. Many of these progresses are based on the advances of nuclear magnetic resonance (NMR) studies of perfused breast cancer cells and tumor-bearing animal models. One of the major limitations of the application of NMR methods both in vitro and in vivo is its low sensitivity. The sensitivity determines the ultimate cancer detection capability and the resolution in image and in spectrum. In this study, a high temperature superconductor (HTS) working at very low temperature will be used to reduce electronic noise and significantly improve the sensitivity of detection. It will dramatically increase the sensitivity and improve the resolutions (37-39). The improvement will be verified by comparing the sensitivity with that of a conventional

probe. The improvement of detection sensitivity will provide a more accurate diagnosis, and it may become possible for early prediction of tumor response to therapy. The probes will be constructed with $YBa_2Cu_3O_7$ material and tested in two well defined experiments: an in vitro cell metabolism study on a 9.4 T spectrometer and an in vivo tumor bearing animal study on a 4.7 scanner. In the cell metabolism study, the breast cancer cell line MCF7 and its variants will be studied in terms of characteristic differences of their ^{31}P spectra during growth phase and under effects of Tamoxifen (40-41). In the in vivo animal study, MCF7 cells and its variants will be grown as xenografts on nude mice. The differences of 31P spectra during progress of tumor and responses to Doxorubicin and Tamoxifen will be studied. The high-resolution proton imaging experiments of vasculature of tumor will also be conducted.

VI. Body

In the first year of the project, the design of self-resonant probes for high-resolution NMR has been completed (Figure 1A and 1B). The receiver coil uses thin-film, high temperature superconductor (HTS), $YBa_2Cu_3O_7$. The transmitter coil is a standard room-temperature coil. The probe is designed to fit either a 9.4 T machine for in vitro cell study or a 4.7 T machine for animal study. The coils are detachable so that different coil can be substituted in and out of the different machines and for different nuclei. Three identical cell perfusion apparatus (Figure 2) for the NMR study of breast cancer cell metabolism have been constructed and tested. The apparatus was tested using known standard compounds. To study the metabolism of breast cancer cells for an extended period of time, the cells are continuously perfused with nutrients. During perfusion, the breast cancer cells are restrained in agarose gel-thread matrices. A protocol for making agarose gel-thread matrices containing MCF7 breast cancer cells is established (Figure 3A and 3B). Besides the above-mentioned tasks, some of the infrastructure and preparation works necessary for conducting the proposed research have been accomplished including relocation of a 400 MHz machine and renovation of laboratories. As part of support, the university has renovated two laboratories for this project. One of the laboratories accommodates the NMR machines. The other laboratory is for the chemical and biological preparation. A large amount of laboratory supplies and cell culture materials have been ordered. New equipment including computers, a refrigerator and a de-ionized water column have been purchased and installed.

In the second year of this project, we have fabricated and tested a HTS coil, as well as, studied the ^{31}P spectroscopic differences of MCF 7 cells and its variants and their responses to Tamoxifen and Doxorubicin. Based on the test done at 77 ^{0}K, the HTS coil has a resonance frequency 401.6 MHz and the Q value for the coil is 650. This is better than expected in the design. We have studied the differences in the ^{31}P NMR spectroscopic profiles for drug sensitive MCF7 cancer cells and their multidrug resistant variant MCF7/ADR cells (42). The cells are embedded in agarose gel threads and perfused with growth medium during the NMR studies. Many detailed phosphorus metabolites have been identified. The peaks on the spectrum associated with phosphoethanolamine (PE), phosphocholine (PC), inorganic phosphate (Pi), glycerophospho-ethanolamine (GPE), glycerophosphocholine (GPC), adenosine triphosphate (ATP) and diphosphodiester (DPDE) can be clearly identified (Figure 4). There may be some subtle differences in the spectra of the MCF7/WT type and

MCF7/ADR cell lines. However, the differences are not conclusive using the conventional probe with the limited resolution. We have successfully demonstrated drug sensitive MCF7 cells, which were dramatically affected by 2 μM Doxorubicin within two hours perfusion (Figure 5) and not responsive to Tamoxifen up to 12 hours (Figure 6). In contrast, 2 μM Doxorubicin was without any effect on multidrug resistant MCF7/ADR cells (Figure 7) and the ^{31}P NMR spectrum did not differ appreciably after addition of Doxorubicin. In order to have a highest S/N in the in vivo studies, a great deal of efforts has been made to ensure a reliable NMR system and a contamination free cell culture environment. The scan parameters are optimized. The magnetic field drift during the long acquisition time is negligible. All the potential cell contamination sources are eliminated.

In the third year, we concentrated on the in vivo animal study. The MCF7 wild type human breast cancer cells and its drug resistant variants were grown as solid tumor xenographs in athymic nude mice as the animal model. This in vivo animal study was a continuation of the vitro cell study. The results from the animal model were used to confirm whether the differences seen in vitro are also observed in the in vivo spectra obtained for the tumors growing in nude mice. The in vivo NMR imaging and spectroscopy studies of the solid tumor have been providing information regarding (i) heterogeneity and microvasculature of tumor, (ii) energy metabolism, (iii) tumor pH, (iv) tumor hypoxia, (v) observed predictive response to antiestrogens and Doxorubicin even before regression by tumormeter measurements.

Besides this in vivo animal study, the integration of the Oxford Spectrostate cryostat with the HTS probe was completed in this year. The whole system includes HTS coil, mounting facilities, the fine-tuning paddle and a copper impedance matching loop and the preamp. We also have procured the specialized cryo-valves, low temperature components and Oxford cryostat. The HTS probe was assembled with the cryostat at Quantum Magnetics Inc (Figure 8). In this year, a localized spectroscopy technique ISIS (image-selected in vivo spectroscopy) and STEAM techniques have been implemented and tested (43-49). The intended selected volume was well defined. To study the progress of tumor a series of the in vivo ^{31}P spectra were taken from MCF7/ADR drug resistant tumor on 4, 6, 8, and 12 days after cell implantation (Figure 9A). The spectra clearly showed the gradual decreases of phosphocreatine and ATP. The spectra also showed the increase of inorganic phosphate. The potential malignant markers such as phosphomonoester and phosphodiester signals were weak. The spectra from the non-involved control leg demonstrated no metabolic changes during this period (Figure 9B). The constant spectral intensities also demonstrate the consistency of the NMR machine. The results from these in vivo ^{31}P spectroscopic studies were similar to the results from the in vitro cell studies. The signal-to-noise ratio of the in vivo animal studies was better. This was primarily due to more cells involved in the in vivo studies. Although all the spectra show excellent signal-to-noise ratio, the measurement of absolute values of each phosphate is difficult. This is primarily due to the NMR setup and detection sensitivity may not be identical every time. It is always a challenge for a quantitative measurement. The contributing factors for the variation in the measurement include coil tuning, sample shimming, RF pulse calibration and the relative position of the animal to the coil. In order to have a consistent reference, methylenediphosphonic acid fixed

on the coil is used as an external reference. This ensures a constant intensity of the reference in the quantitative measurements of the metabolites.

In the third year, we also studied the small blood vessels of mice using NMR microscopic imaging technique. The purpose of this study is to examine density and the relative leakiness of capillaries in tumors. The field-of-view is 1.5 cm x 1.5 cm. The in-plane spatial resolution was 30 μm. A series of high quality detailed images revealed small blood capillaries near a wound could easily be identified (Figure 10).

For the fourth year, we continued the in vivo spectroscopy study. We had constructed an improved cell perfusion system (Figure 11). The improved cell perfusion system contained both a negative pressure and a positive pressure part before and after the pump (50-51). These negative and positive pressure parts helped with the removal of air bubbles in the medium. They also served as reservoirs to trap the air. An air bubble trapped in the NMR tube would cause magnetic field inhomogeneity and, consequently, degrade the quality of the spectrum. Using the improved perfusion system, the proposed cell metabolism studies could be extended to a much longer time, more than 8 days. In the previous study, the experiment could only run up to 14 hours. With this improved perfusion system, many time consuming experiments can be performed more reliably and the signal-to-noise ratio has been dramatically improved.

For the in vivo spectroscopy study, MCF7/WT (wild type) breast cancer cells ($\sim 10^8$) were grown as conventional monolayers and harvested as single cell suspensions, which were then embedded in agarose gel threads. These cells embedded in agarose threads were transferred to a NMR tube and then perfused with culture medium using the new perfusion system. Figure 12 shows an improved NMR spectrum. Phosphorus metabolites peaks are well separated and can be easily identified. The spectrum is an accumulation of 1800 transients and the repetition time is 2 seconds. The line broadening used is 10 Hz. The signal-to-noise ratio is significantly better than the results in the beginning of the project (see Figure 4). The line width of the γ-ATP peak is 50 Hz. The ^{31}P NMR spectrum can be deconvoluted. Each individual component of phosphorus metabolites can be separated from the spectrum (Figure 13). The individual peak-height and the integral under the peaks can be calculated and listed as in the inserted table. The differences between the original spectrum and the fitted curve shown on the bottom of the figure indicate the decomposition of the peaks is complete.

Since the signal-to-noise ratio of the NMR spectrum is usually low, sometimes a long scan time is needed. This long data acquisition time prevents some fast changing experiments such as drug effects on the metabolism of breast cancer cells. With the improved perfusion system, long term in vivo study becomes feasible. Figure 14 shows a long term in vivo ^{31}P NMR spectroscopy study of MCF7 breast cancer cells. A series of ^{31}P spectra over 5 days was obtained. Each spectrum is an accumulation of 3 hours, 5370 transients and 2 seconds repetition time. The line broadening is 10 Hz. Only every other spectrum is shown in Figure 14. The changes of each phosphorus metabolites can be easily studied. During this time, PC, GPE and GPC increases while other phosphorus metabolites stay constant. Changes of individual phosphorus metabolites of MCF7/WT (wild type) cells over first 72 hours are carefully studied. Figure 15 shows the concentrations of 6 out of 11 phosphorus metabolites: PE, PC, GPE, GPC and DPDE. During the first 72 hours, GPE and GPC continuously

increase while PE and DPDE remains constant. The PC peak increases initially and it approaches a plateau later. The increases of GPE and GPC indicate the cell proliferation. Figure 16 shows the concentrations of another five phosphorus metabolites α-ATP, β-ATP, γ-ATP, PCr, and Pi. During the course of study, ATP and Pi continuously grow and PCr remains constant.

With the improved NMR perfusion system four drug sensitivity studies were conducted using iodoacetamide, rotenone, sodium azide and barbital with different concentrations. The purposes of these drug sensitive studies are to assess (a) the metabolic process on ATP production by cells (b) the importance of oxidative phosphorylation on ATP production and (c) the availability of oxygen in the perfusion system. 10^8 MCF7/WT breast cancer cells embedded in the agarose gel were first perfused with growth medium. After the system is stabilized (~2 hours after perfusion with medium), a series of 42 one-hour ^{31}P NMR spectra were taken. Each spectrum contains 1700 transients with 1 second repetition time. Drug concentrations from 0.1mM to 10 mM were used. For the iodoacetamide study, after 17 hours baseline scans, 1mM iodoacetamide was added in the perfused medium. Figure 17 and Figure 18 shows the phosphorus metabolites concentrations plotted as functions of time. Six metabolites are in Figure 17 and the other five metabolites are in Figure 18. Figure 17 shows the absolute concentration changes of the PE, PC, GPE, GPC and DPDE. After perfusion with iodoacetamide, PE increases dramatically and then decreases. GPE and GPC show slight increases initially and decreases afterwards. DPDE shows continuous decreases. In Figure 18, it shows the other five phosphorus metabolites: α-ATP, β-ATP, γ-ATP, intra- and extra-cellular Pi. After perfusion with iodoacetamide, ATP increases slightly and then decreases. The rates of decreasing GPE, GPC, DPDE and ATP depend on the concentrations of iodoacetamide. Iodoacetamide is an inhibitor of the electron transport chain and consequently it will change the respiratory states of the cells. While the concentrations of high-energy phosphates decreases, the intracellular Pi continuously increases. A new extracellular Pi peak appears immediately after the drug perfusion and the concentration of the extracellular Pi increases for a few hours before it disappears due to the perfusion. The ability of detection of extracellular Pi and separated from the intracellular Pi after exposure to different drugs is new and exciting. For barbital study (10 mM) the ATP and PCr signals dropped 50% and then stabilized. There are no effects using rotenone and sodium azide up to 10 mM.

The NMR T1 relaxation times of all the phosphorus metabolites of MCF7 breast cancer cells were measured with the improved NMR perfusion system. Since some of the T1 of the phosphorus metabolites are long, the T1 measurement has been always difficult in the past. It requires a long measurement time. The T1 measurement of the phosphorus metabolites becomes feasible only with the improved perfusion system. A saturation recovery technique has been used for the T1 measurement in this study (Figure 19). A series 16 RF pulses flips the magnetization to horizontal plane first. It follows by a 90^0 RF pulse and the data acquisition. The measured T1 relaxation times for each phosphorus metabolites are listed in the table in the Figure 19. The T1 values vary from 0.38 seconds for β-ATP to 12 seconds for GPE.

For the in vivo study, cancer cell suspensions ($5x10^6$ cells) from monolayer cultures in the exponential phase of growth are injected into the left hind leg of mice subcutaneously.

The tumor-free right hind leg of the mouse was used as control. The cancer cells are grown as solid tumor xenographs (Figure 20). For the in vivo imaging, a surface coil is gently placed around the tumor. The mouse is anesthetized by i.p. injection of katamine and xylazine. A set of T1 and T2 weighted images throughout the tumor were obtained first. Then, MRI contrast agent Magnevist (Berlex Laboratories, Wayne, NJ) was injected intravenously. Figure 21 shows two images of the tumor before and after the contrast injection. Clearly, there is a significant image enhancement in the tumor. The bright area in the image indicates the presence of contrast agent. The degree of enhancement is different throughout the tumor, which reflects the heterogeneity of tumor. For the MCF7 tumor model, no significant vascular structure can be identified in the core of tumor. There is a significant signal enhancement at peripheral that indicates plenty of blood supply on the surface of tumor.

Key Research Accomplishments

I. Probe Design

- Detail the design of high temperature superconductor (HTS) probe for 9.4T NMR machine.
- Procure specialized cryo-valves and low temperature mechanical and electrical components.
- Fabricate the components of HTS probe and assemble the probe.
- Construct a conventional copper probe for comparison.
- Evaluate components and test the operation characteristics of HTS probe. The Q value of the HTS probe is 650.

II. Cell Metabolism Study

- Design and construct a perfusion apparatus and perfect the perfusion experiment, eliminate the air bubble and magnetic field drift problems during the perfusion study.
- Establish a protocol, which significantly extend the useful experiment time, for in vitro NMR study of cancer cells using the new perfusion system.
- Obtain ^{31}P spectra of MCF7 wild type and drug resistant breast cancer cells. The NMR signals of phosphorus metabolites from MCF7 cells are well separated. The identifiable phosphorus metabolites include phosphoethanolamine (PE), phosphocholine (PC), inorganic phosphate (Pi), glycerophosphoethanolamine (GPE), glycerol-phosphocholine (GPC), phosphocreatine (PCr), γ-adenosine triphosphate (γ-ATP), α-adenosine triphosphate (α-ATP), diphosphodiester (DPDE), and β-adenosine triphosphate (β-ATP).
- During the prolonged in vitro study of MCF7 breast cancer cells perfuse with IMEM medium, PC, GPE and GPC increase while other phosphorus metabolites stay constant. The increases of GPE and GPC indicate the cell proliferation.
- Drug sensitive MCF7 wild type cells were dramatically affected by 2 μM Doxorubicin within two hours perfusion and not responsive to Tamoxifen up to 12 hours. In contrast, 2 μM Doxorubicin was without any effect on the drug resistant MCF/ADR cells.
- To determine the lowest number of cells in agarose, $5x10^6$, which still can have a good SNR in a reasonable acquisition time (3600 scans, 2 hours).

- The T1 relaxation times of each phosphorus metabolites of MCF7 cells ranging from 0.38 sec for β-ATP to 12 sec for GPE were measured first time. The measurement becomes feasible due to the improved perfusion system, which is sustainable for long scan time.
- When the MCF7 breast cancer cells treated with mitochondria poisons such as iodoacetamide (1 mM), PE, GPE, GPC and ATP slightly increase initially and then decreases in 10 hours while DPDE continuously decrease. There is a new extracellular Pi peak appears immediately after perfusion of iodoacetamide. The extracellular Pi peak increases first while the intracellular Pi peak decreases indicating the leakage of intracellular Pi into extracellular space. The ability of detection of extracellular Pi and separated from the intracellular Pi signal is a novelty.

III. In Vivo Animal Study

- In vivo ^{31}P NMR spectroscopy has shown many phosphorus metabolites in tumors grown on nude mice. There is a significant lower PCr and ATP signals and higher Pi in the tumor than in the normal control leg muscle.
- A series of in vivo NMR spectroscopy studies during tumor growth indicates gradual decreases of PCr and ATP and increases of Pi. This indicates there is relatively more nonviable narcotic tissue in the tumor as tumor progresses.
- A localized NMR spectroscopy technique has implemented, which provides biochemical information from various sections in the tumor. Although, it has a relative poorer sensitivity, it does provide information from a more specific area within the tumor. The localized spectroscopic signals shows higher Pi and lower PCr and ATP at the core of tumor compared to the nonselective signals from the entire tumor.
- A high resolution MRI protocol (in-plan resolution, 30 μm) has been established for imaging of blood vessels in a mouse. New small capillaries near a wound have been identified. There is no identifiable blood vessel inside the MCF7 tumor.
- Using a T1 weighted spin-echo imaging technique with MRI contrast agent, Magnevist, the internal structure of tumor was studied. A significant image enhancement occurred at the peripheral of tumor after i.v. injection of contrast agent but not at the core of tumor. Higher image intensity indicates higher contrast agent and higher blood supply at the peripheral.

Reportable outcomes

1. A list of manuscripts, abstracts and presentations supported by this award:

- Agwu, EC, Sridhar R, Wang PC. In vitro and In vivo Characterization of MCF7 Multidrug Resistant Cell Metabolism Using Magnetic Resonance Spectroscopy. 3rd Annual Research Forum, Howard University, Washington, DC. December 10, 1999.
- Wang PC. Biomedical Applications of Nuclear Magnetic Resonance Imaging and Spectroscopy. Symposium on Recent Trends in Physics. FuJen University, Taipei, Taiwan, November 27, 1999
- Wang PC, Liu DS, Agwu EC, Sridhar Rajagopalan. Application of P31 NMR Spectroscopy to Distinguish Drug Sensitive and Drug Resistant Breast Cancer. Era of Hope. pp.217, 2000.

- Zhou JW, Agwu CE, Li EC, Wang PC. An Improved NMR Perfusion System For Breast Cancer Cell Study. 42nd Experimental NMR Conference, March 11-16, Orlando, FL. 2001.
- Agwu, EC, Zhou JW, Sridhar R, Wang PC. An Improved NMR Perfusion System For Breast Cancer Cell Study. 15th Annual Scientific Meeting, October 12-14, Washington, DC. 2001.

2. Design and construct a superconductor RF probe with Q value 650.
3. An improved cell perfusion system has been constructed for in vivo NMR study to extend the in vivo study from 14 hours to longer than 8 days.
4. Five postdoctoral fellows, Drs. Dongsheng Liu, Chi Yuling, Zhou Jienwei, Huafu Song, and Rengsu Zhang and a MD/PhD student Mr. Emmanuel Agwu were supported by this grant. Mr. Agwu intends to finish his Ph.D. thesis by the end of 2001 and his M.D. training by year 2002. Two of the postdoctoral fellows went to industry. One took a teaching position in a university. The other two postdoctoral fellows continue employment in this lab as a lab manager and a research associate.
5. Two U.S. Army training grants have been received based on this research:

- "MR Sensitivity Improvement Using High Temperature Superconductor for RF Probe" (DAAG55-98- 1-0187)
- "A Training Program in Breast Cancer Research Using NMR Techniques" (DAMD- 17-00-1-0291)

VII. Conclusions

In this project we have constructed and tested a high temperature superconductor RF coil and a conventional RF probe to study phosphorus metabolites in MCF7 breast cancer cells and tumor bearing animals. The Q value of this HTc coil (resonance frequency 401.6 MHz) at 77^0K is 650. We have studied the differences in the ^{31}P NMR spectroscopic profiles for drug sensitive MCF7 breast cancer cells and their multidrug resistant variant MCF7/ADR cells. The cells are embedded in agarose gel threads and perfused with growth medium during the NMR studies. Many phosphorus metabolites have been identified including: phosphoethanolamine (PE), phosphocholine (PC), inorganic phosphate (Pi), glycerophospho-ethanolamine (GPE), glycerophosphocholine (GPC), phosphocreatine (PCr), γ-adenosine triphosphate (γ-ATP), α-adenosine triphosphate (α-ATP), diphosphodiester (DPDE), and β-adenosine triphosphate (β-ATP). There are some subtle differences in the spectra of the wild type and multidrug resistant cells. The GPC signal is higher than PC signal for drug sensitive cells. However, for the drug resistant cells, GPC is lower than PC signal. We have also successfully demonstrated that the drug sensitive MCF7 cells were dramatically affected by 2 μM Doxorubicin within two hours perfusion and not responsive to Tamoxifen up to 12 hours. In contrast, 2 μM Doxorubicin was without any effect on multidrug resistant MCF7/ADR cells and the ^{31}P NMR spectrum did not differ appreciably after addition of Doxorubicin. We have constructed an improved cell perfusion system. Using the improved perfusion system the duration of the cell metabolism studies has been extended more than 8 days much longer than the previously reported 14 hours. This long and stable study significantly improved the signal-to-noise ratio of the NMR spectrum. The T1 relaxation times (ranging from 0.38 sec to 12 sec) of each phosphorus metabolites of MCF7 cells were measured first time. With these

sustainable long scans, some of the entwined peaks, particularly in the PE/PC, GPE/GPC, and intra- and extra-cellular Pi regions, can be well separated. Four MCF7 breast cancer cells drug sensitivity studies were also conducted. Mitochondria poison drugs (iodoacetamide, rotenone, sodium azide, and barbital) with different concentrations (0.1-10 mM) were perfused through the NMR tube containing the cancer cells. For MCF7/WT cancer cells treated with iodoacetamide, PE, GPE, GPC and ATP show a slight increase initially and a decrease later while DPDE continuously decreases. In addition to the intracellular Pi peak, an extracellular Pi peak appears immediately after perfusion of iodoacetamide. The extracellular Pi indicates the leakage of intracellular Pi into extracellular space. The ability of detection of extracellular Pi and separation from the intracellular Pi signal is exciting. For barbital, ATP and PCr signals dropped 50% and then stabilized. There are no effects using rotenone and sodium azide up to 10 mM.

For the in vivo animal studies, NMR spectroscopy and imaging techniques were used on tumor bearing nude mice. In vivo ^{31}P NMR spectroscopy has shown many phosphorus metabolites similar to that in the cancer cell studies. There is significantly lower PCr and ATP signals and higher Pi in the tumor than in the normal control leg muscle. During tumor growth PCr and ATP gradually decreases and Pi increases. This indicates there is relative more nonviable narcotic tissue in the tumor as tumor progresses. A localized NMR spectroscopy technique has implemented, which provides biochemical information from various sections in the tumor. Although it has a relative poorer sensitivity due to smaller tissue volume, the localized spectrum does provide information from a more specific area within the tumor. The localized spectroscopic signals shows higher Pi and lower PCr and ATP at the core of tumor compared to the nonselective signals from the entire tumor. For NMR imaging of tumor, a high resolution MRI protocol has been established with in-plan spatial resolution 30 μm. New small capillaries near a wound have been identified. There is no identifiable blood vessel inside the MCF7 tumor. Using a T1 weighted spin-echo imaging technique with MRI contrast agent, Magnevist, the internal structure of tumor was studied. A significant image enhancement occurred at peripheral and a small part of the tumor after i.v. injection of contrast agent. The enhancement is not uniform, which reflects the heterogeneity of the tumor. Higher image intensity indicates higher contrast agent and higher blood supply at the peripheral.

VIII. REFERENCES

1. Kopan, DB. Breast Imaging. Philadelphia: Lippincott, 1989.
2. Ferenezy A, Winkler B. Blaustern's Pathology of the Female Genital Tract (ed. Kuman RJ) p218, Springer –Verlag. New York, 1987.
3. Degani H. Spectroscopy of Cells. 8th International Soc. for Magn. Res. Med. April, 2000.
4. Michal Neeman, Hadassa Degani Metabolic Studies of Estrogen- and Tamoxifen-treated Human breast Cancer Cells by Nuclear Magnetic Resonance Spectroscopy. Cancer Research 49, 589-594. 1989.
5. Stelling CB, Wang PC, Lieber A, etal, Prototype coil for magnetic resonance imaging of the female breast, Radiology 154(2): 457-62,1985.
6. Harms SE, Flaming DP, Present and Future Role of MR imaging, Syllabus; A categorical

Course in Physics Technical Aspects of Breast Imaging RSNA, 1992.
7. Harms SE, Flaming DP, MR imaging of the breast, J. Mag. Res. Imaging 3:277-283, 1993.
8. Harms SE, Flaming DP, Hesley KL, etal, Magnetic Resonance Imaging of the breast, Mag. Res. Quarterly, 8(3):139-155, 1992
9. El Youself SJ, O'Connell DM, Magnetic resonance imaging of the breast, Mag. Res. Annual, 177-195, 1986.
10. Kuelson MH, El Youseif SJ, Goldberg RE, Ballance W, Intracustic Papillary Carcinoma of the breast: mammographic, sonographic and MR appearance with pathologic correlation, J. Comp. Ass. Tomography 11(6):1074-1076, 1987.
11. Partain CL, Kulkarni MV, et al, Magnetic resonance imaging of the breast: Functional T1 and Three-dimensional Imaging, Cardio Vas, Intervent, Radiology 8:292-299, 1986.
12. Santyz GE, Henkelman M, Bronskill M, Spin-locking for magnetic resonance imaging with application to human breast, Mag. Res. Med. 12:25-27, 1989.
13. Adams AH, Brookeman JR, Merickel MB, Breast lesion discrimination using statistical analysis and shape mesures on MRI, Compt. Med. Imaging and Graphics 15(5):339-349, 1991.
14. Harms SE, Flamig DP, Hesley KL, Evans WP, Cheek JH, Ptters GN, Knox SM, Savino DA, Netto GJ, Wells RB, Jones SE. Fat-suppressed Three-dimensional MR Imaging of the Breast,RadioGraphics 13:247-267, 1993.
15. Fischer U, Vosshenrich R, Probst A, Burchhardt H,Grabbe E, Preoperative MR-mammography in diagnosed breast carcinoma, Rofo-Fortschr Geb Rontgenstr Neuen Bildgeb Verfahr 161 (4):300-306 1994.
16. Kuhl C, Specificity of dynamic contrast-enhance MR mammography, Syllabus of Workshop in Breast MR, Soc. Magnet. Reson. p5 June 1995.
17. Vogl, T., Peer, F., Schedel, H., Reiman, V., Holtmann, S., Rennschmid, C., Sauter, R., and Lesner, J. ^{31}P-spectroscopy of head and neck tumors - Surface coil technique. Magn. Reson. Imaging 7, 425-435 (1989).
18. Koutcher, J.A., Ballon, D., Graham, M., Healey, J.H., Casper, E.S., Heelan, R., and Gerweck, L.E. ^{31}P NMR spectra of extremity sarcomas: diversity of metabolic profiles and changes in response to chemotherapy. Magn. Reson. Med. 16, 19-34 (1990).
19. Shinkwin, M.A., Lenkinski, R.E., Daly, J.M., Zlatkin, M.B., Frank, T.S., Holland, G.A., and Kressel, H.Y. Integrated magnetic resonance imaging and phosphorous spectroscopy of soft tissue tumors. Cancer 67, 1849-1858 (1991).
20. Glaholm, J., Leach, M.O., Collins, D.J., Mansi, J., Sharp, J.C., Madden, A., Smith, I.E., and McCready, V.R. In vivo ^{31}P magnetic resonance spectroscopy for monitoring treatment response in breast cancer. Lancet I, 1326-1327 (1989).
21. Ng, T.C., Grundfest, S., Vijayakumar, S., Baldwin, N.J., Majors, A.W., Karalis, I., Meaney, T.F., Shin, K.H., Thomas, F.J., and Tubbs, R. Therapeutic response of breast carcinoma monitored by ^{31}P MRS in situ. Magn. Reson. Med. 10, 125-134 (1989).
22. Twelves, C.J., Lowry, M., Porter, D., Graves, P., Smith, M.A., and Richards, M.A. ^{31}P MR spectroscopy of breast cancer in vivo: metabolite characteristics and influence of estrogen receptor status and tumor grade. Soc. Mag. Res. Med. Abstr., p. 1216 (1990).
23. Kalra, R., Hands, L., Styles, P., Wade, K., Greenall, M., Smith, K., Harris, A., and Radda, G.K. Localized ^{31}P spectroscopy of human breast cancer correlations of phosphomonoester and phosphodiester with epiderman growth factor expresion. Soc.

Mag. Res. Med. Abstr., p. 1217 (1990).
24. Redmond, O.M., Stack, J.P., O'Connor, N.G., Codd, M.B., and Ennis, J.T. In vivo phosphorous ^{31}P magnetic resonance spectroscopy of normal and pathological breast tissue. Br. J. Radiology 65, 210-216 (1991).
25. Aisen, A.M., and Chenevert, T.L. MR spectroscopy: clinical perspective. Radiology 173, 593-599 (1989).
26. Bottomley, P.A. Human in vivo NMR spectroscopy in diagnostic medicine: Clinical tool or research probe? Radiology 170, 1-15 (1989).
27. Daly, P.F., and Cohen, J.S. Magnetic resonance spectroscopy of tumors and potential in vivo clinical applications: A review. Cancer Res. 49, 770-779 (1989).
28. Glickson, J.D. Clinical NMR spectroscopy of tumors. Invest. Radiol. 24, 1011-1016 (1989).
29. den Hollander, J.A., Luyten, P.R., Marien, A.J.H., Segebarth, C.M., Baleriaux, D.F., de beer, R., and Van Ormondt, D. Potentials of quantitative image-localize human ^{31}P nuclear magnetic resonance spectroscopy in the clinical evaluation of intracranial tumors. Mag. Reson. Quarterly 5, 152-168 (1989).
30. Radda, G.K., Rajagopalan, B., and Taylor, D.J. Biochemistry in vivo: An appraisal of clinical magnetic resonance spectroscopy. Mag. Reson. Quarterly 5, 122-151 (1989).
31. Steen, R.G. Response of solid tumors to chemotherapy monitored by in vivo ^{31}P nuclear magnetic resonance spectroscopy: A review. Cancer Res. 49, 4075-4085 (1989).
32. Vaupel, P., Kallinowski, F., and Okunieff P. Blood flow, oxygen and nutrient supply, and metabolic microenvironment of human tumors: A review. Cancer Res. 49, 6449-6465 (1989).
33. Negendank W, Studies of Human Tumors by MRS: a Review, NMR Biomed. 5:303-324 1992.
34. Bhujwalla ZM, Shungu DC, He Q, Wehvle JP, Glickson JD. MR Studies of Tumors: Relationship between Blood Flow, Metabolism and Physiology. NMR in Physiology and Biomed. P311-328, Academic Press. 1994.
35. Howe FA, Maxwell RJ, Saunders DE, Brown MM, Griffiths JR. Proton Spectroscopy In Vivo Magnet. Reson. Quarterly, 9(1):31-59, 1993.
36. Mountford CE, Lean CL, Mackinnon WB. The Use of Proton MR in Cancer Pathology. Ann. Report on NMR Spect. 27:173-215, 1993
37. R.D. Black, T.A. Early, P.B. Roemer, O.M. Mueller, A Mogro Campero, L.G. Turner, G. A. Johnson. A High-Temperature Superconducting Receiver for NMR Microscopy. Science 259:793-795, 1993.
38. D.I. Hoult and R.E. Richards, "The signal-to-noise ratio of the nuclear magnetic resonance experiment," J.Mag.Res. 24, 71-85, 1976.
39. Black R.D., P.B. Roemer, W.A. Edelstein, S.P. Souza, A. Mogro Campero, L.G. Turner, Scaling Laws and Cryogenic Probes for NMR Microscopy in Proceedings of the Tenth Annual Meeting of the Soc. Magn. Reson. Med. San Fransisco, CA, August 10-16, 1991.
40. Mimnaugh, E.G., Fairchild, C.R., Fruehauf, J.P., and Sinha, B.K. Biochemical and pharmacological characterization of MCF-7 drug-sensitive and Adr^R multidrug resistant human breast tumor xenografts in athymic nude mice.Bichem. Pharmacol. 42:391-402, 1991.
41. Cohen, J.S., Lyon, R.C., Chen, C., Faustino, P.J., Batist, G., Shoemaker, M., Rubalcaba, E. and Cowan, K.H. Differences in phosphate metabolite levels in drug-sensitive and

resistant human breast cancer lines determined by ^{31}P magnetic resonance spectroscopy. Cancer Res. 56:4087-4090, 1986.
42. Wang PC, Liu DS, Agwu EC, Sridhar Rajagopalan. Application of P31 NMR Spectroscopy to Distinguish Drug Sensitive and Drug Resistant Breast Cancer. Era of Hope. pp.217, 2000.
43. Garwood, M. Introduction to Basic Principles of Spectral Localization. Syllabus,11th Ann. Meeting, Soc. Mag. Res. Med. p. 222-231, 1992.
44. R.J. Ordidge, M.R. Bendall, R.E. Gordon, and A. Connelly, Magnetic resonance in biology and medicine (Govil, Khetrapal, and Saran, Eds.), p.387, Mcgraw-Hill, New Delhi, 1985.
45. Bottomley PA, Hardy CJ, Roemer RB, Weiss RG, Problems and expediencies in human 31P spectroscopy, The definition of localized volumes, dealing with saturation and the technique-dependence of quantification NMR in Biomedicine, 2:284-289, 1989.
46. Granot J, Selective volume excitation using stimulated echoes (VEST), Applications to spatially localized spectroscopy and imaging, J. Magn. Res. 70,488-492 (1986).
47. Kimmich R and D. Hoepfel, Volume selective multipulse spin-echo spectroscopy, J. Magn. Reson. 72, 379 (1987).
48. Frahm J, K.D. Merboldt, and W. Hanicke, Localized proton spectroscopy using stimulated echoes, J. Magn. Reson. 72, 502 (1987).
49. Ordidge RJ, A. Connelly, and J.A.B. Lohman, Image selected in vivo spectroscopy (ISIS), A new technique for spatially-selective NMR spectroscopy, J. Magn. Reson. 66, 283 (1986).
50. Zhou JW, Agwu CE, Li EC, Wang PC. An Improved NMR Perfusion System For Breast Cancer Cell Study. 42nd Experimental NMR Conference, March 11-16, Orlando, FL. 2001.
51. Agwu, EC, Zhou JW, Sridhar R, Wang PC. An Improved NMR Perfusion System For Breast Cancer Cell Study. 15th Annual Scientific Meeting, October 12-14, Washington, DC. 2001.

IX. Appendices

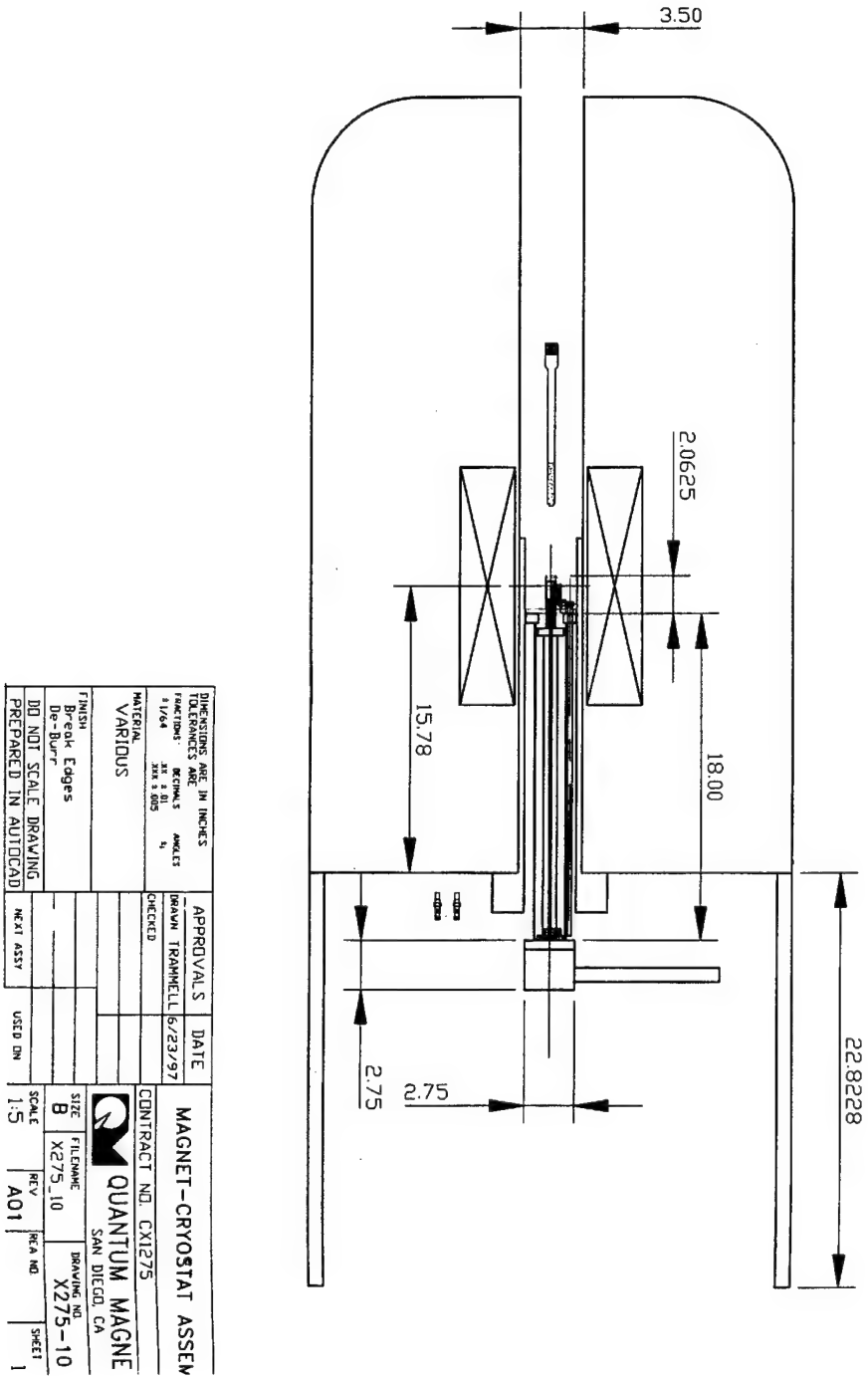

Figure 1A. A side view of the high temperature superconductor probe in the XL-400 NMR machine. The HTS probe is loaded from the bottom of the magnet.

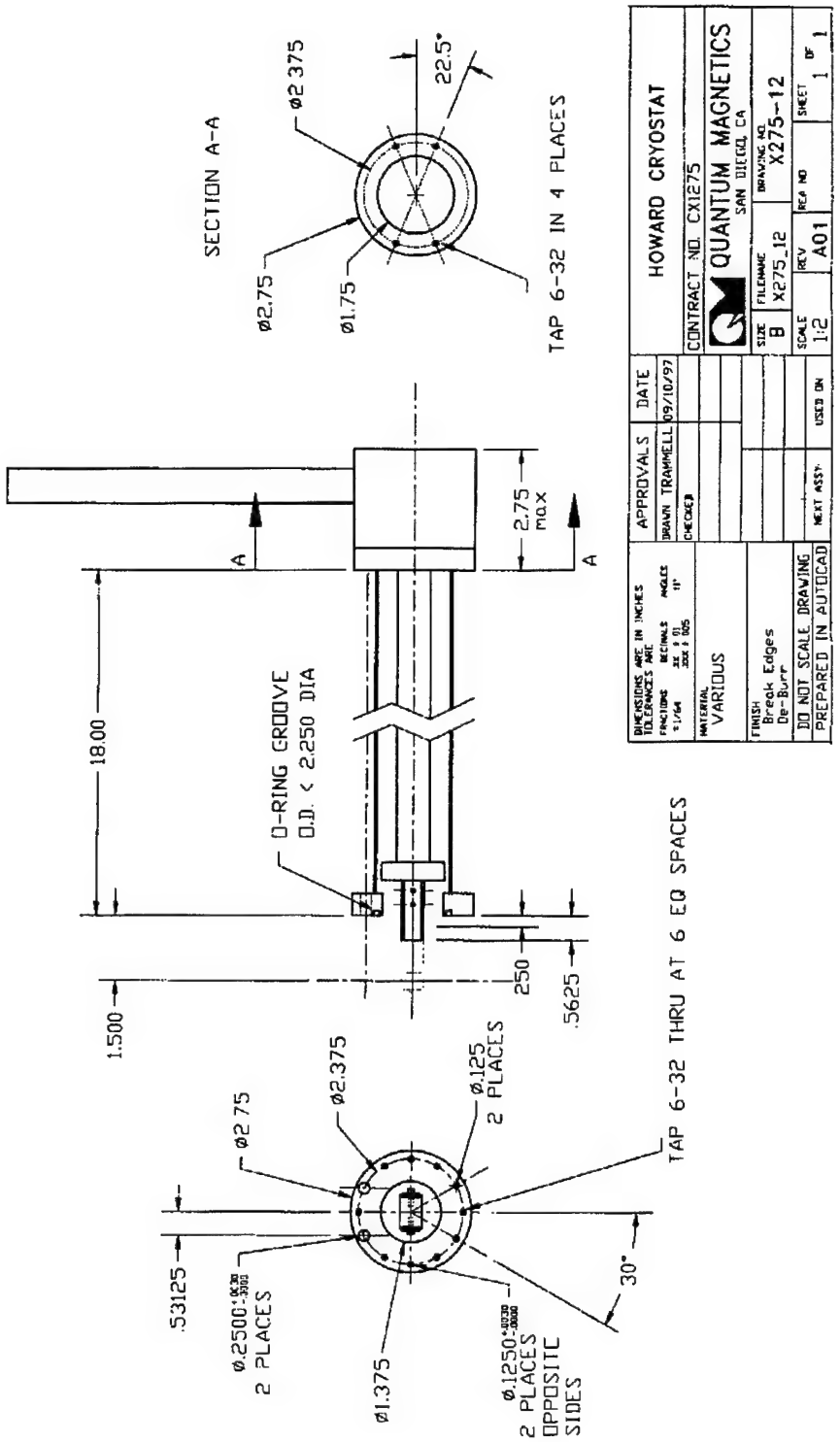

Figure 1B. A detailed drawing (side view and top view) of the cryostat of the HTS probe. This is the insert section, which goes into the magnet from the bottom of the magnet as shown in Figure 1A.

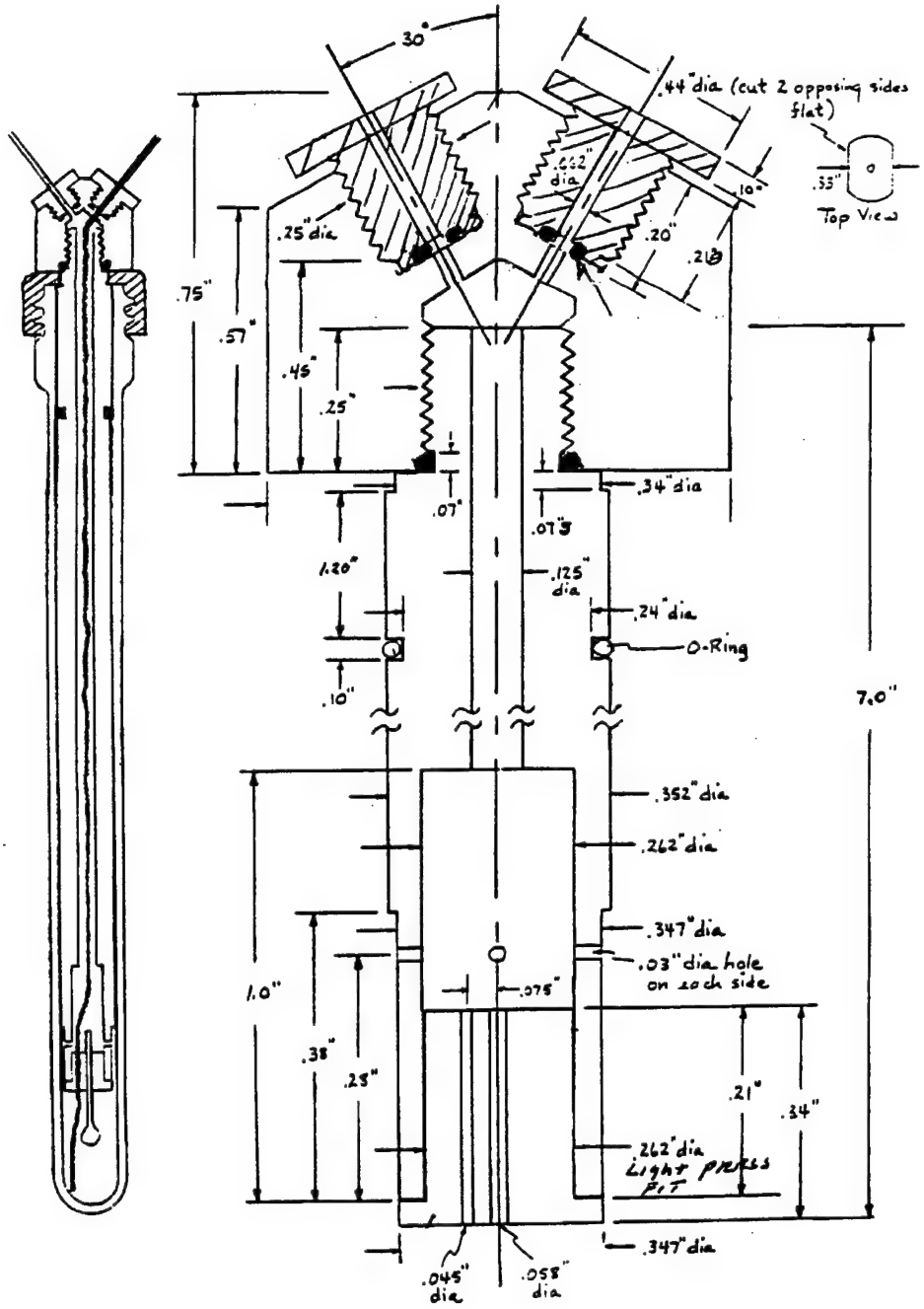

Figure 2. A detailed design for the cell perfusion apparatus. A schematic drawing of the apparatus in a NMR test tube is shown on the left.

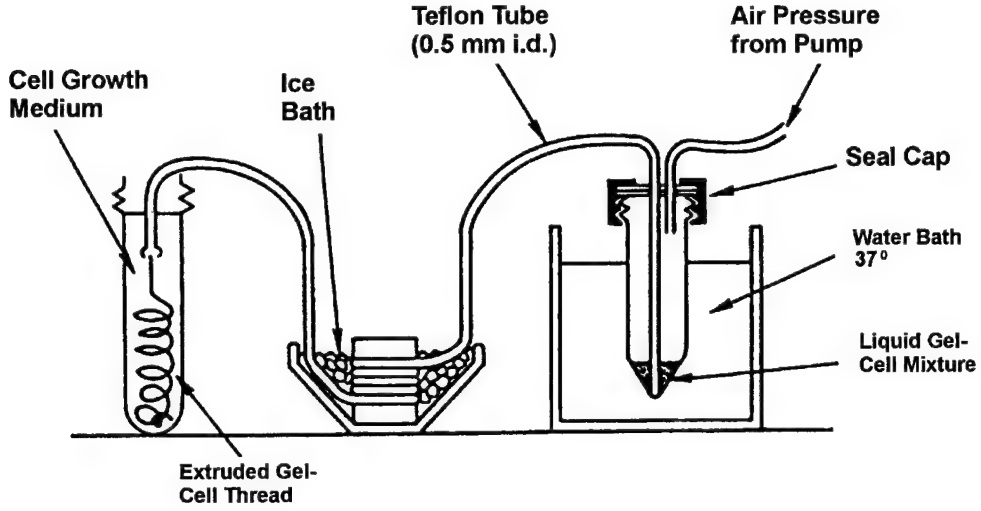

Figure 3A. A diagram of the apparatus for making agarose gel-thread containing breast cancer cells. A mixture of cancer cells with agarose solution is extruded through a fine Teflon capillary tubing chilled by ice. The gel-thread is formed in the tubing and it is forced out directly into the medium is a 10-nm NMR tube ready for perfusion.

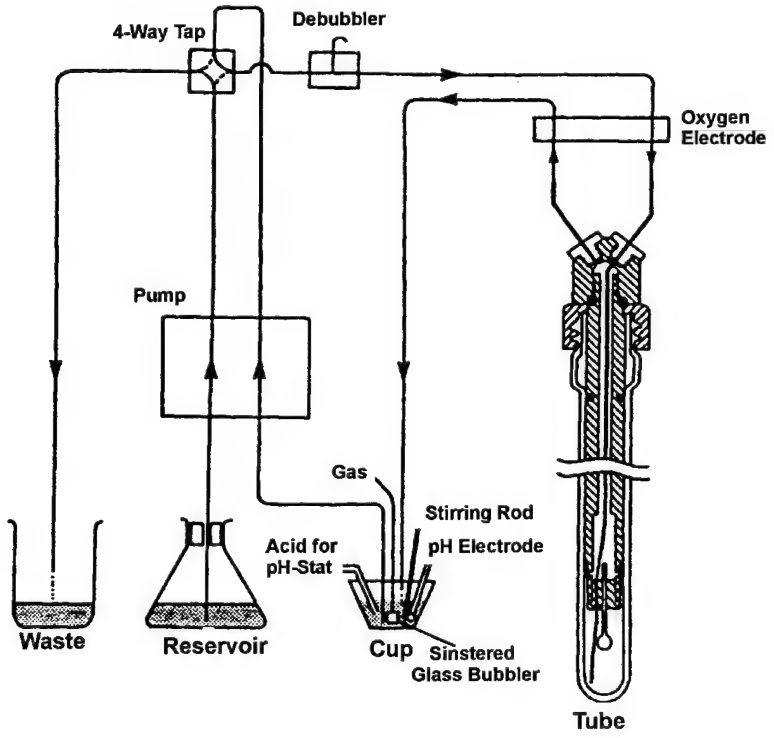

Figure 3B. A schematic diagram of the perfusion system. The figure shows the Kel-F plastic insert in a NMR tube and the flow direction of the perfusion medium.

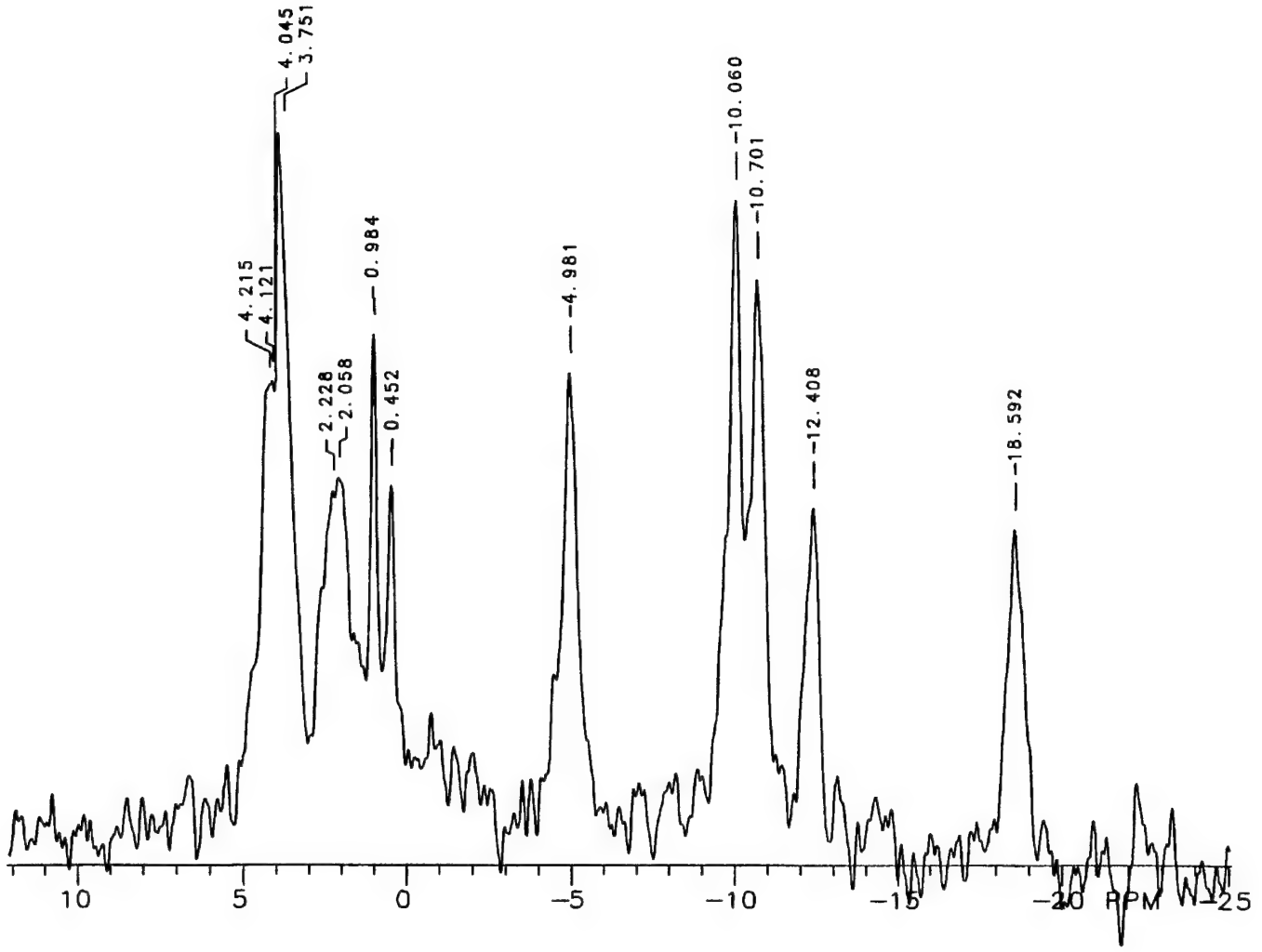

Figure 4. A ^{31}P spectrum of MCF7 wild type cells. The cells are embedded in agarose gel threads perfused with complete growth medium. Many phosphorus metabolites can be identified such as: phosphocholine (PC, 3.75 ppm); inorganic phosphate (Pi, 1.5 2.67 ppm); γ-ATP (4.98 ppm); α-ATP (-10.06 ppm); β-ATP (-18.59 ppm); diphosphodiesters (DPDE, -10.7 plus -12.41 ppm), glycerophosphoethanolamine (GPE, 0.98 ppm) and glycerophosphocholine (GPC, 0.45 ppm).

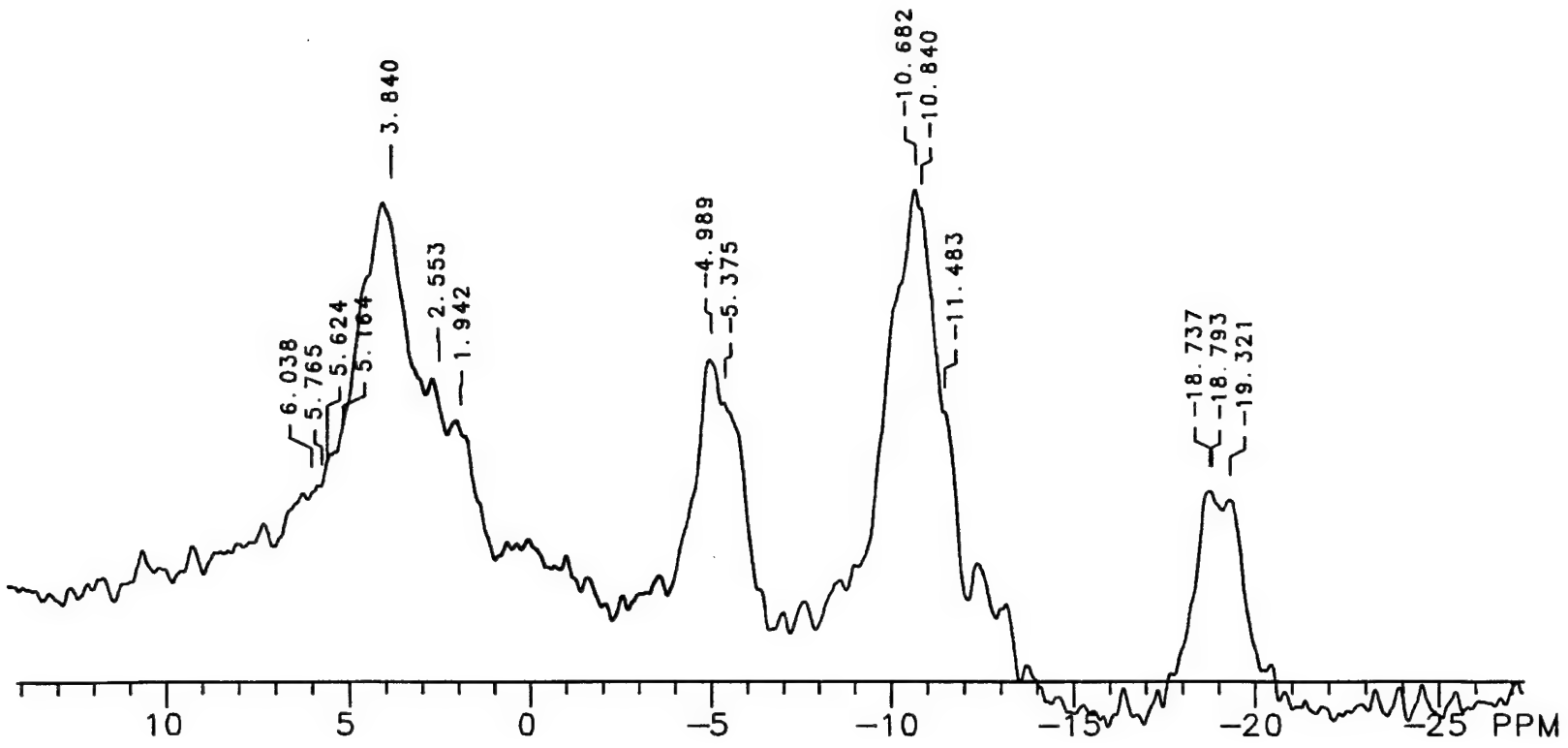

Figure 5. A ^{31}P spectrum of drug sensitive MCF7 wild type cells treated with 2 μM Doxorubicin for 10 hours. The repetition time is 1 second. The number of transient is 2400. The RF pulse width 55 μs. The repetition time is 1 second. The spectrum is an accumulation of 10 hours. The ATP peaks are down and the Pi peak increases.

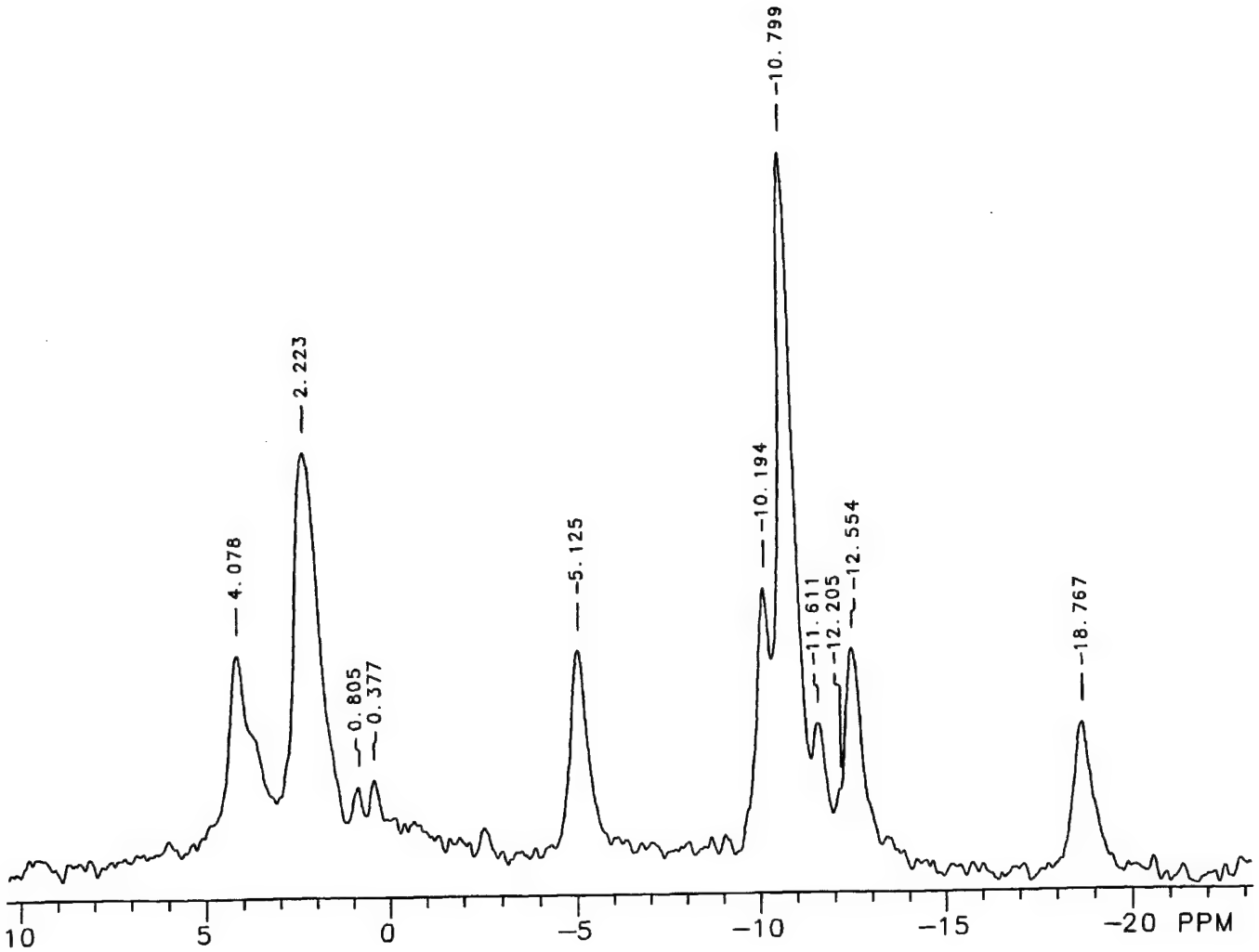

Figure 6. A ^{31}P spectrum of drug sensitive MC7 wild type cells treated with Tamoxifen (8 μg/ml). The repetition time is 1 second. The number of transient is 2000. The RF pulse width is 36.1 μs. There is no difference compared with a spectrum taken from a Tamoxifen free medium.

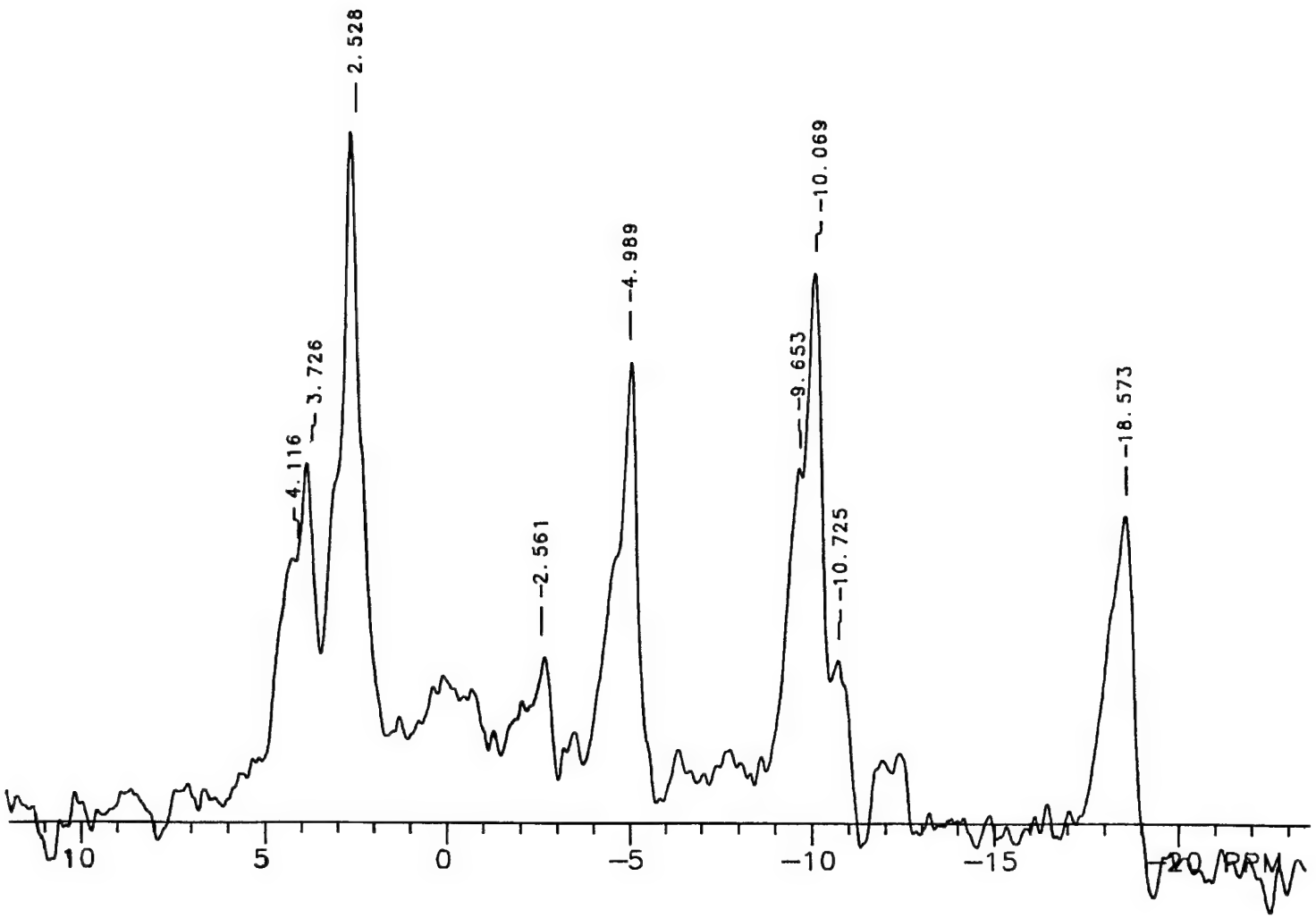

Figure 7. A ^{31}P spectrum of drug resistant MCF7/ADR cells. The perfusion medium contains 2 μM Doxorubicin. There is no change in ATP compared to the spectrum taken before Doxorubicin was introduced. The total scan time was 12 hours. All the scan parameters are the same as in Figure 5.

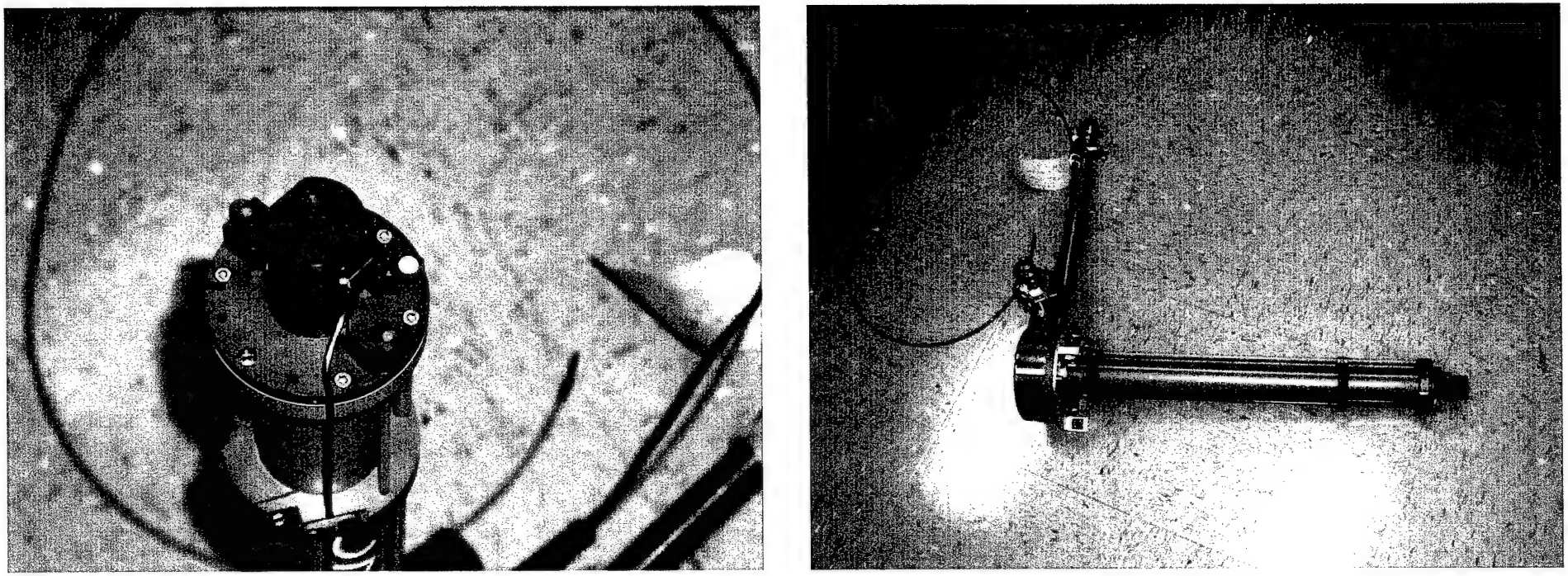

Figure 8. A picture of the complete high temperature superconductor NMR probe assembly including HTS coil and the Oxford Spectrostate Cryostat. This is completed by the subcontractor Quantum Magnetics, Inc. (San Diego, CA).

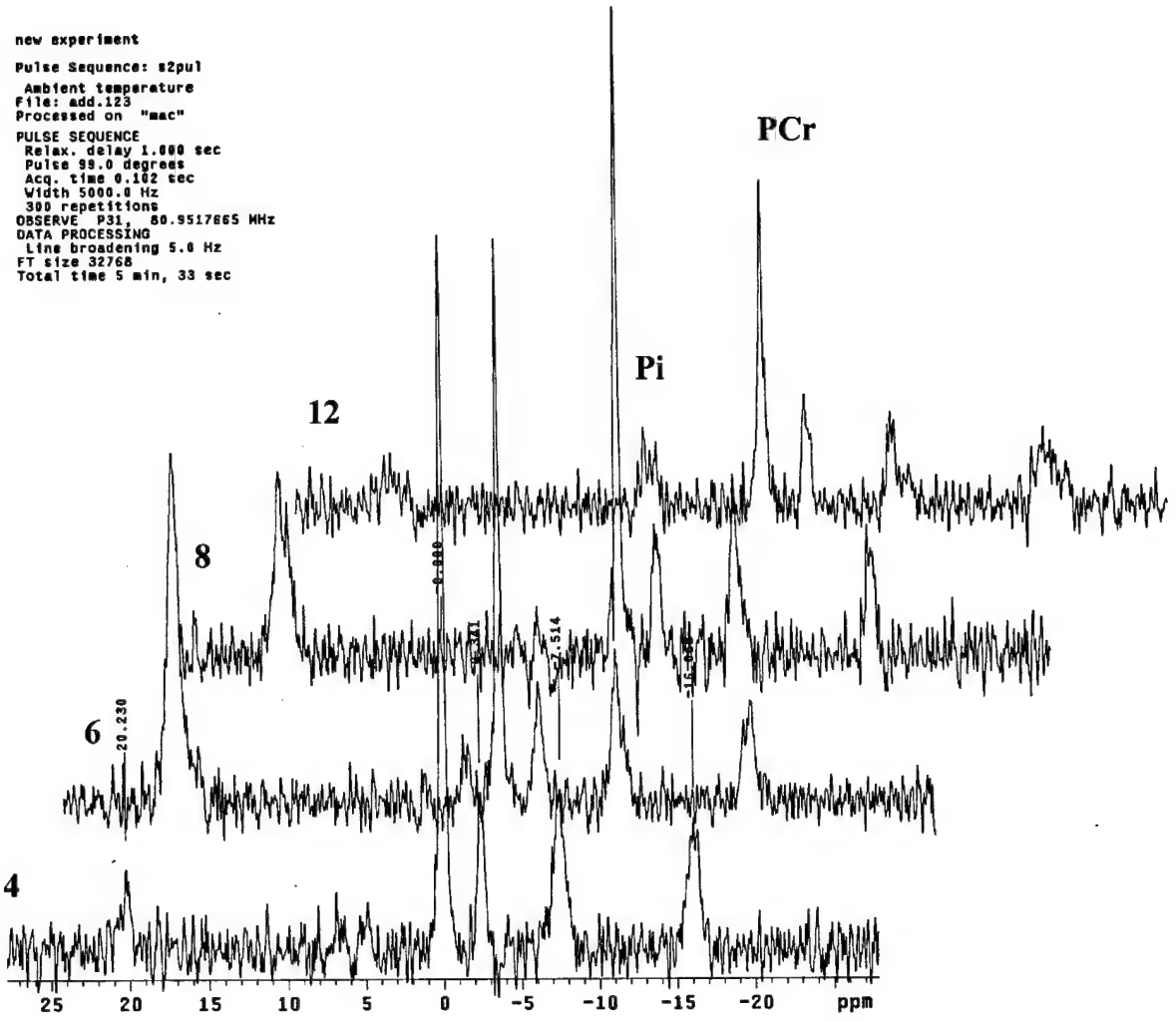

Figure 9A. A series of in vivo NMR spectra (day 4, 6, 8, 12) from a tumor grown by implanting $5x10^6$ MCF7/ADR drug resistant cells on the left hind leg. The phosphate metabolites such as Pi (5.04 ppm), PCr (0 ppm), γ-ATP (-2.34 ppm), α-ATP (-7.51 ppm), and β-ATP (-16.07 ppm) can clearly be identified. The overall high energy phosphates both PCr and ATP gradually dropped at the same time the inorganic phosphate continued to increase. The peak at 20.23 ppm is from an external reference, methylenediphosphonic acid.

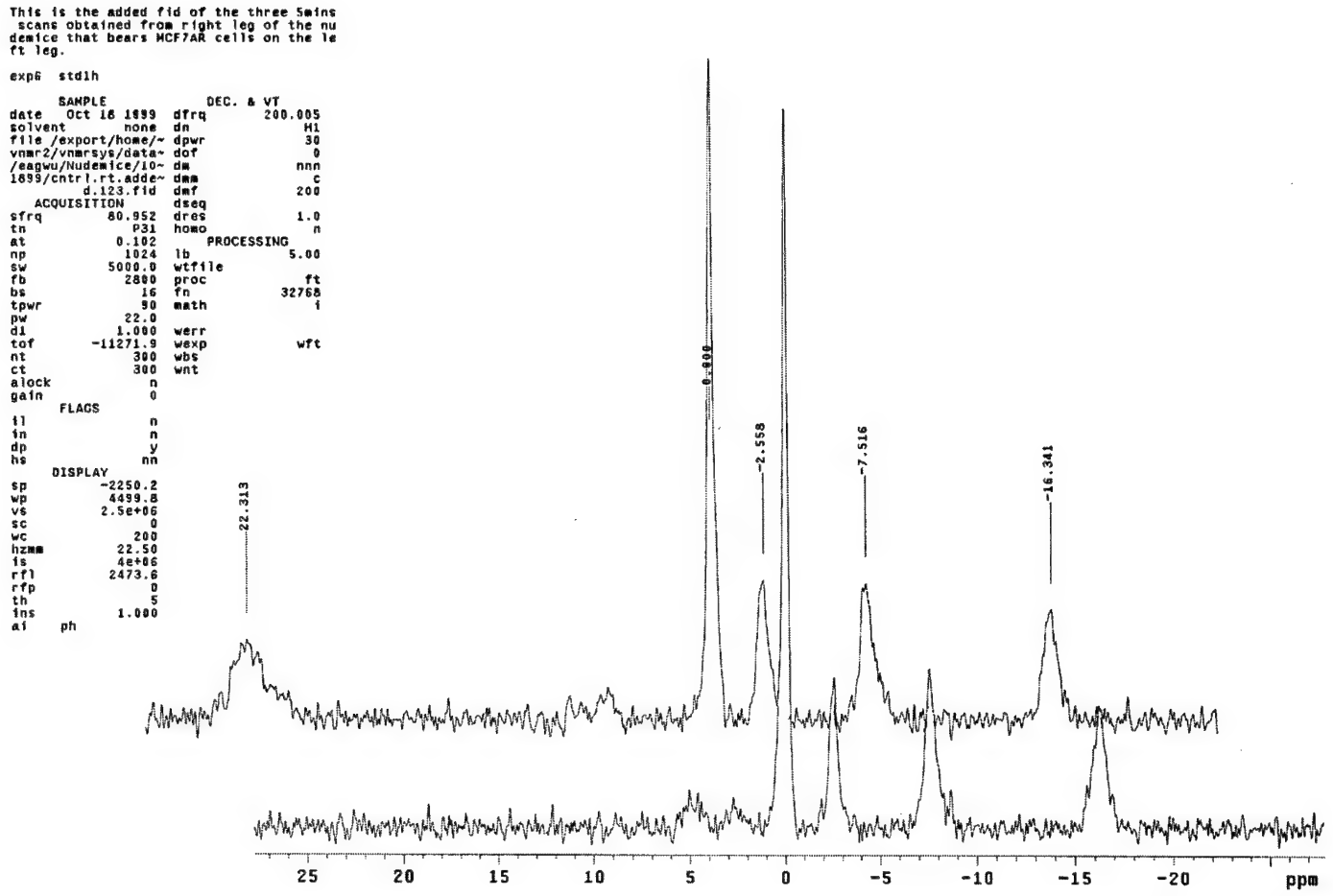

Figure 9B. Two spectra form the tumor-free right hind leg of the mouse on the 4th and 12th day. This serves as a control. The overall signal-to-noise ratio is better than that of the tumor. PCr and ATP signals are stronger. Pi can barely be detected. The intensity does not change during this period of time.

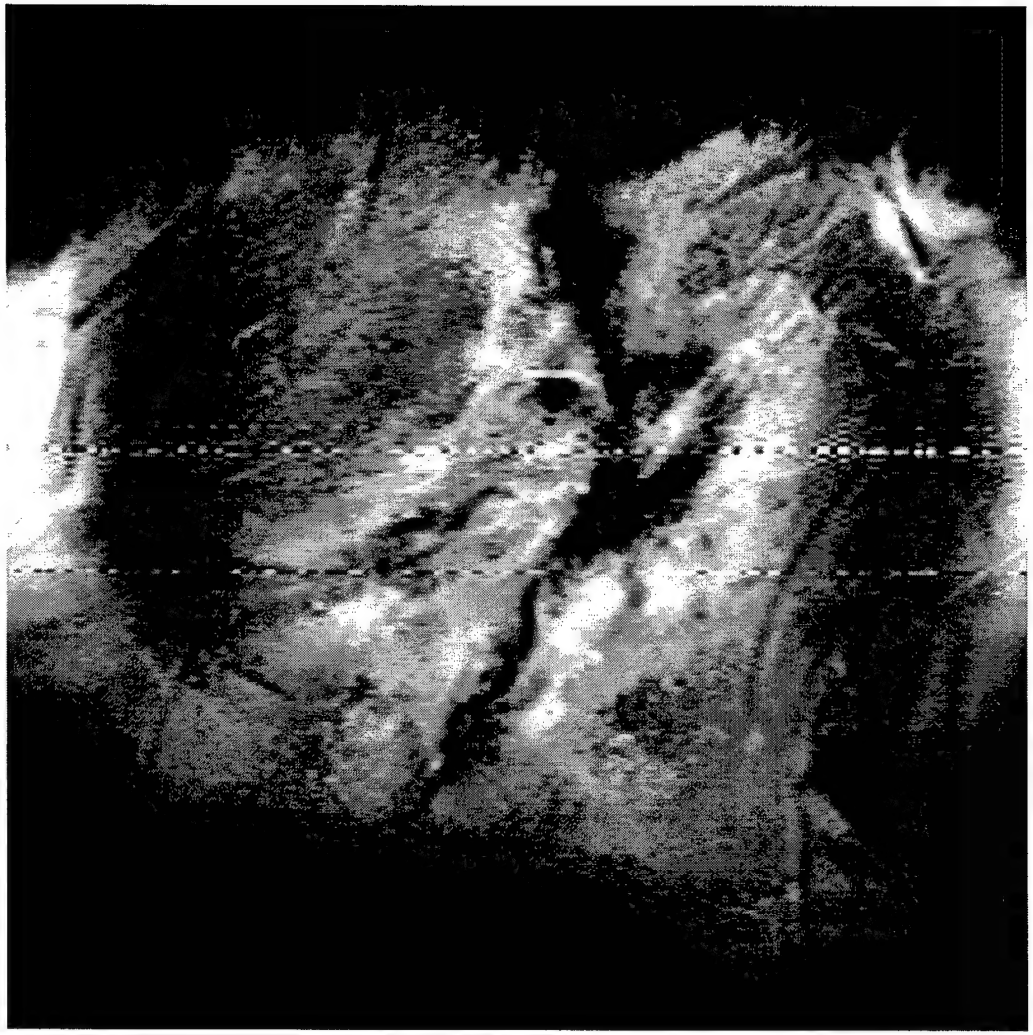

Figure 10. An NMR microscopic image of small blood vessels of mouse. This is a spin-echo image. The repetition time is 1 second and the echo time is 22 μsecond. The field-of-view is 1.5 cm x 1.5 cm. The number of phase encoding steps is 512. The spatial resolution is ~30 μm. The dark lines in the image indicate the small blood vessels.

A Long time perfusion system for Breast Cancer Cells

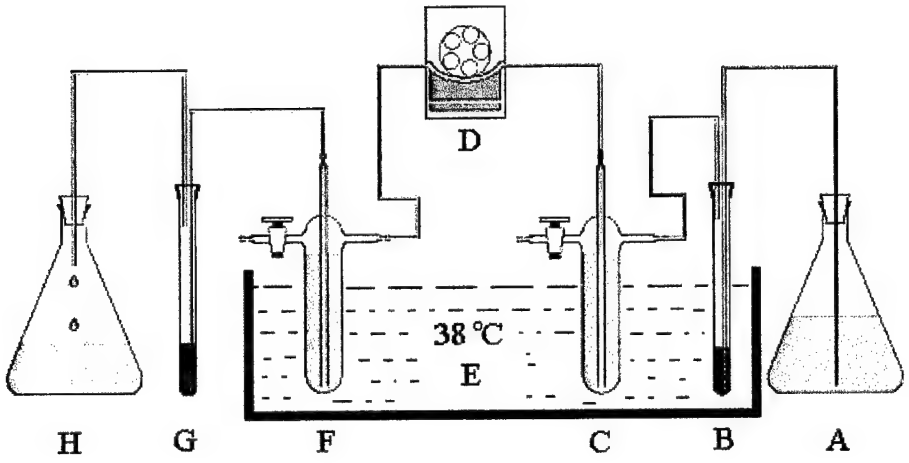

Figure 11. An improved cell perfusion system. (A) medium reservoir (B) gas release inducer (C) gas trap (D) pump (E) gas trap (F) NMR tube (G) waste collector.

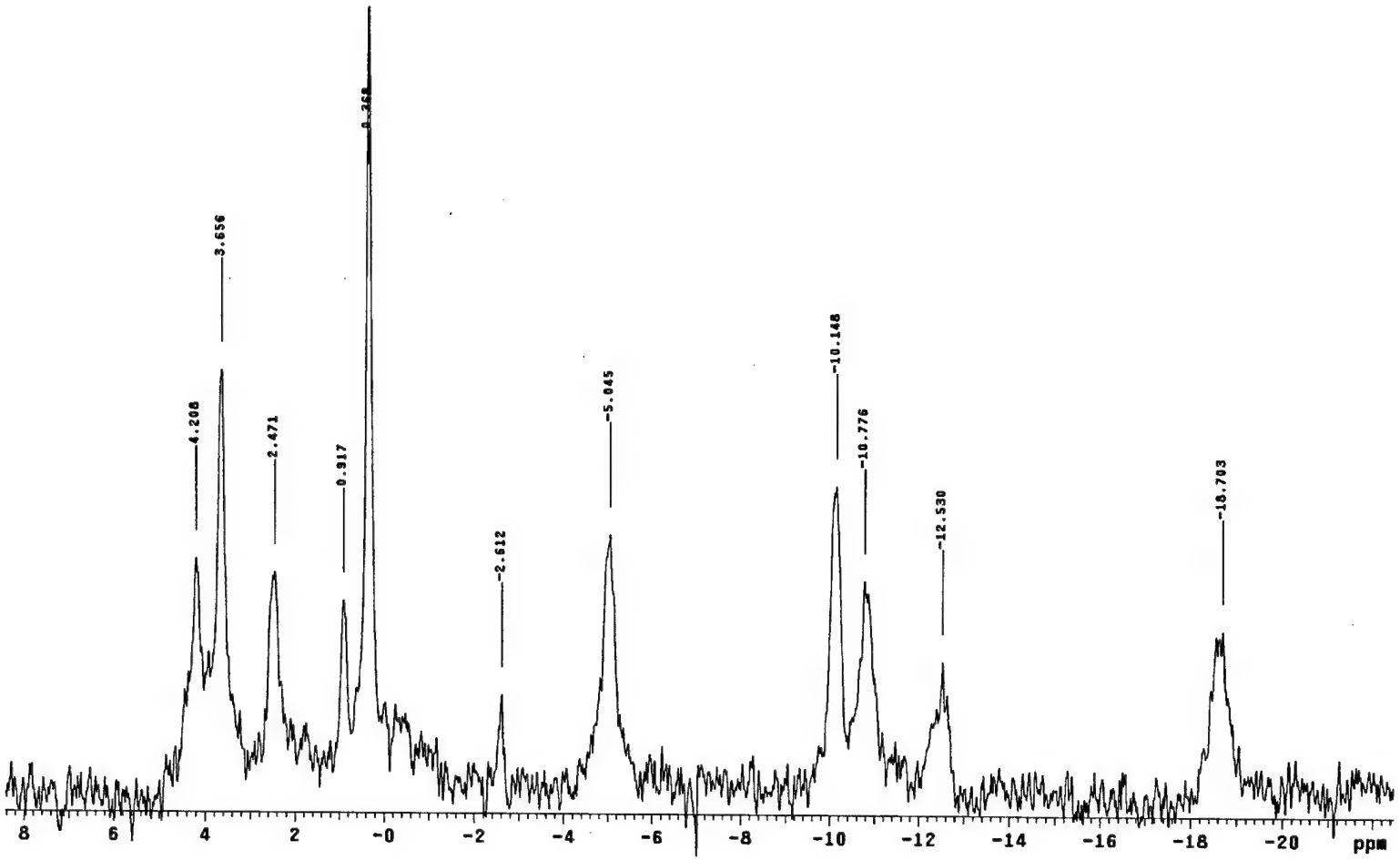

Figure 12. A ^{31}P NMR spectrum of a wild type MCF7 breast cancer cells (10^8 cells) embedded in agarose gel threads. Phosphorus metabolites, including phosphoethanolamine (PE, 4.21 ppm), phosphocholine (PC, 3.66), inorganic phosphate (Pi, 2.47), glycerophosphoethanolamine (GPE, 0.92), glycerophosphocholine (GPC, 0.37) phosphocreatine (PCr, -2.61), γ-adrinophosphate (γ-ATP, -5.05), α-adrinophosphate (α-ATP, -10.15), diphosphodiester (DPDE, -10.78, -12.53), and β-adrinophosphate (β-ATP, -18.70), can be easily identified. The spectrum is an accumulation of 1800 transients and the repetition time is 2 seconds. The signal-to-noise ratio is significantly better than the results in the second report (Figure 4). The line width of the γ-ATP peak is 50 Hz.

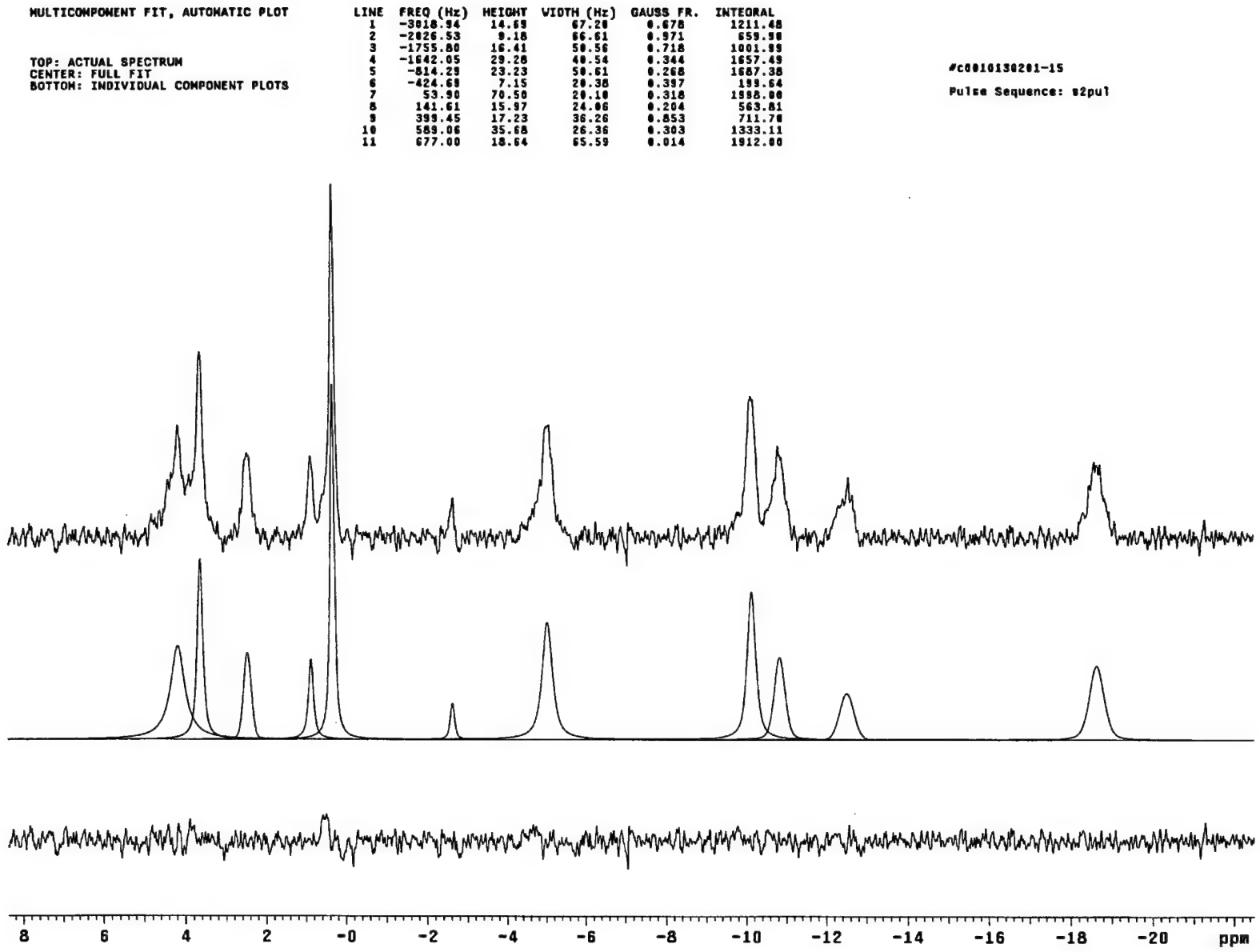

Figure 13. (A) Deconvolution of the ^{31}P NMR spectrum from the Figure 12. (B) Individual phosphorus metabolite peaks that have been separated from the original spectrum. The individual peak-heights and the integrals under the peaks can be derived and are listed in the inserted table. (C) The differences between the original spectrum and the fitted curve.

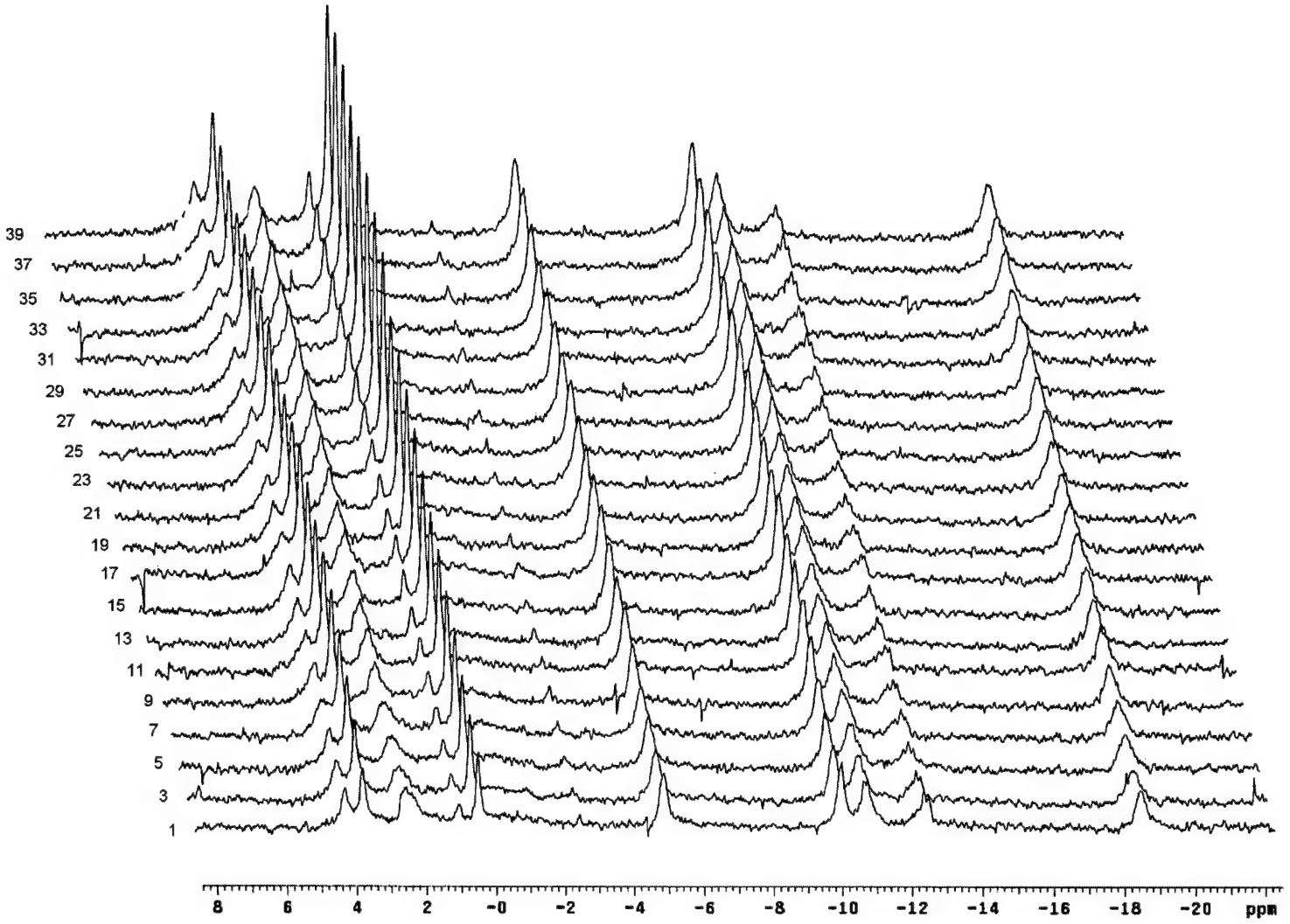

Figure 14. A long term in vivo ^{31}P NMR spectroscopy study of MCF7 breast cancer cells. A series of 47 ^{31}P spectra over 5 days were obtained. Each spectrum is an accumulation of 3 hours, 5370 transients and 2 seconds repetition time. The changes of each phosphorus metabolites can be easily studied. During this time, PC, GPE and GPC increases while other phosphorus metabolites stay constant.

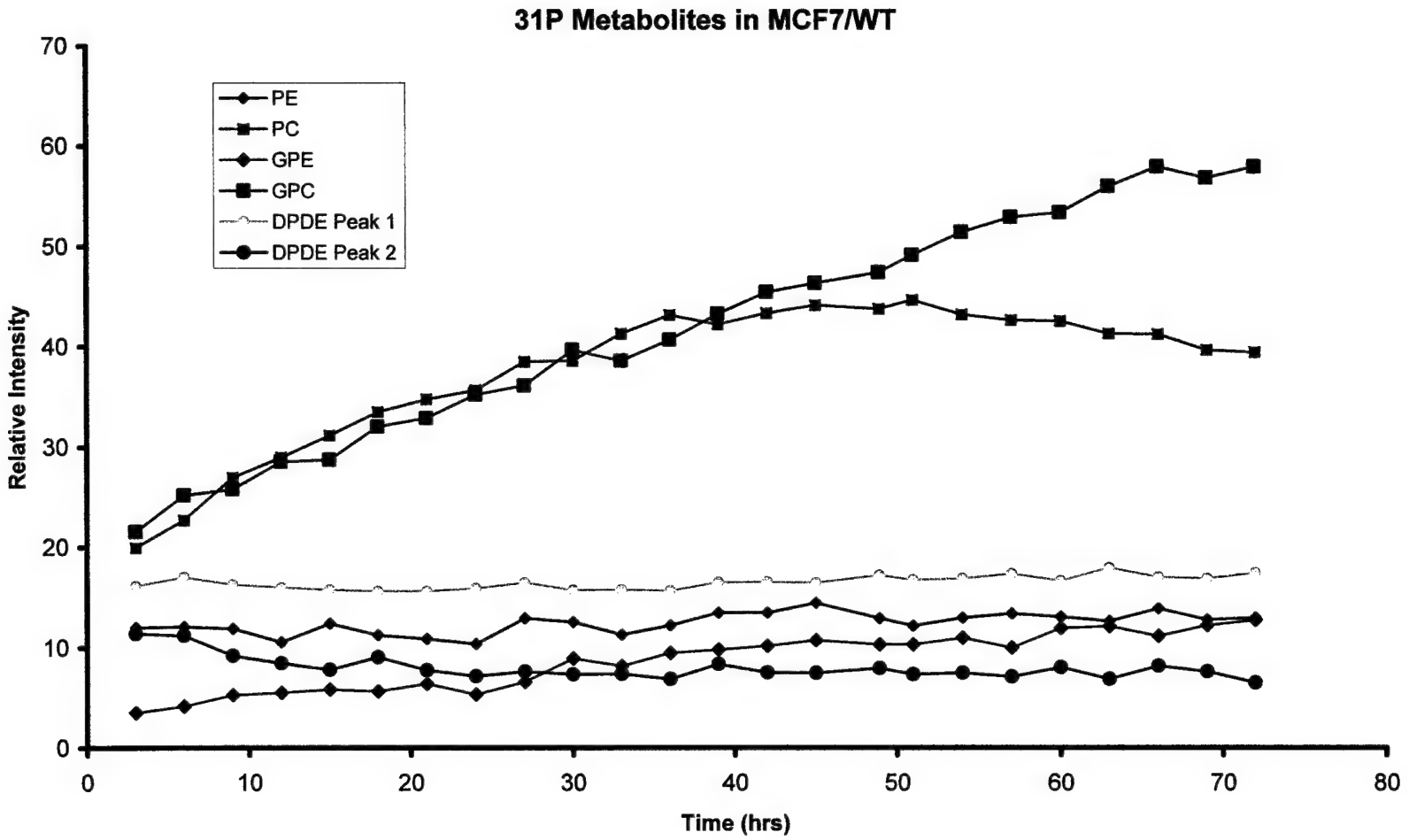

Figure 15. Changes of individual phosphorus metabolites of MCF7/WT (wild type) cells over first 72 hours in a long in vivo study described in Figure 14. This figure contains only 6 out of 11 phosphorus metabolites: PE, PC, GPC and DPDE. The absolute concentrations of the metabolites are plotted as functions of time.

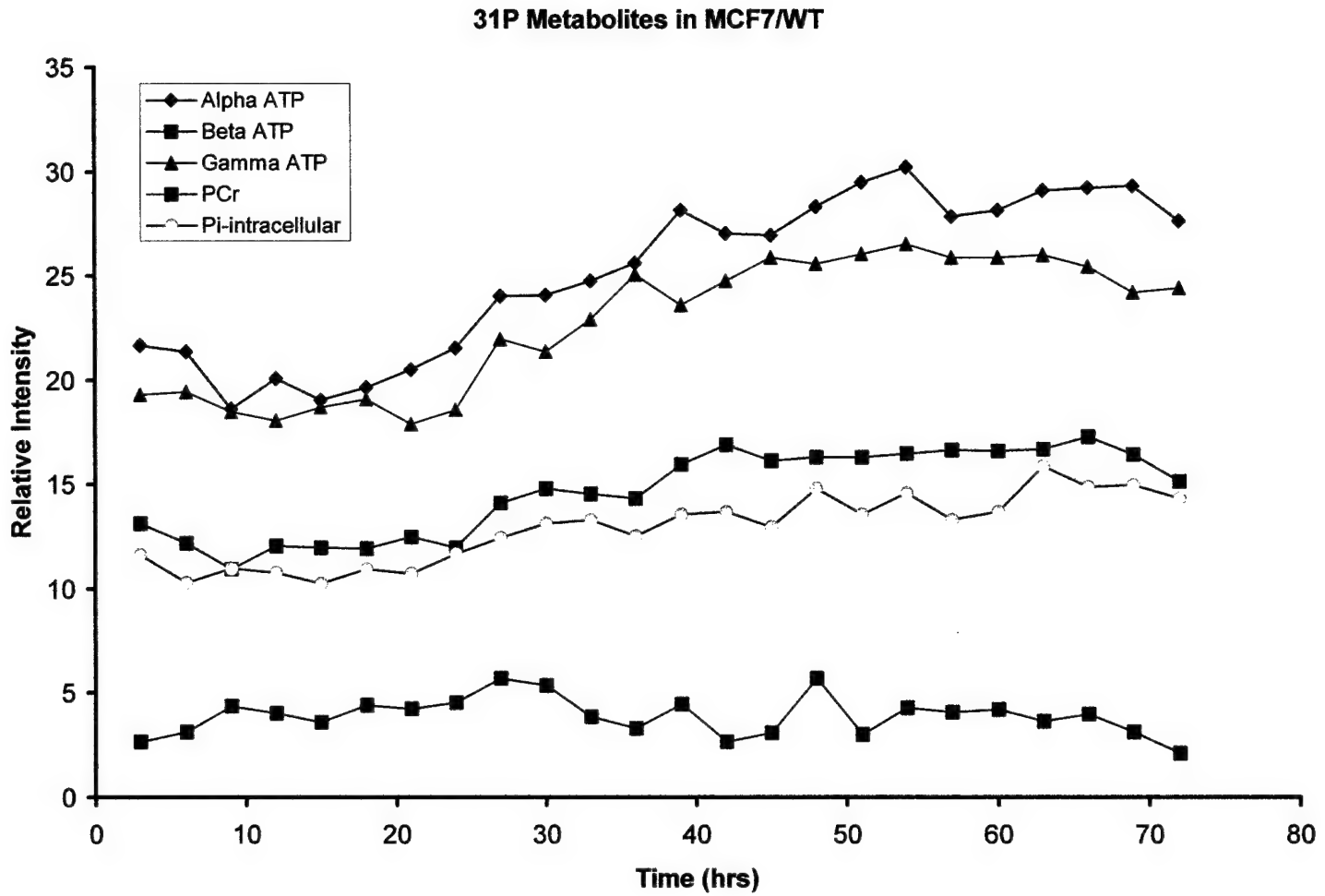

Figure 16. Changes of individual phosphorus metabolites of MCF7/WT cells over first 72 hours from a long in vivo study described in Figure 4. The concentrations of another five phosphorus metabolites α-ATP, β-ATP, γ-ATP, PCr, and Pi are plotted as functions of time.

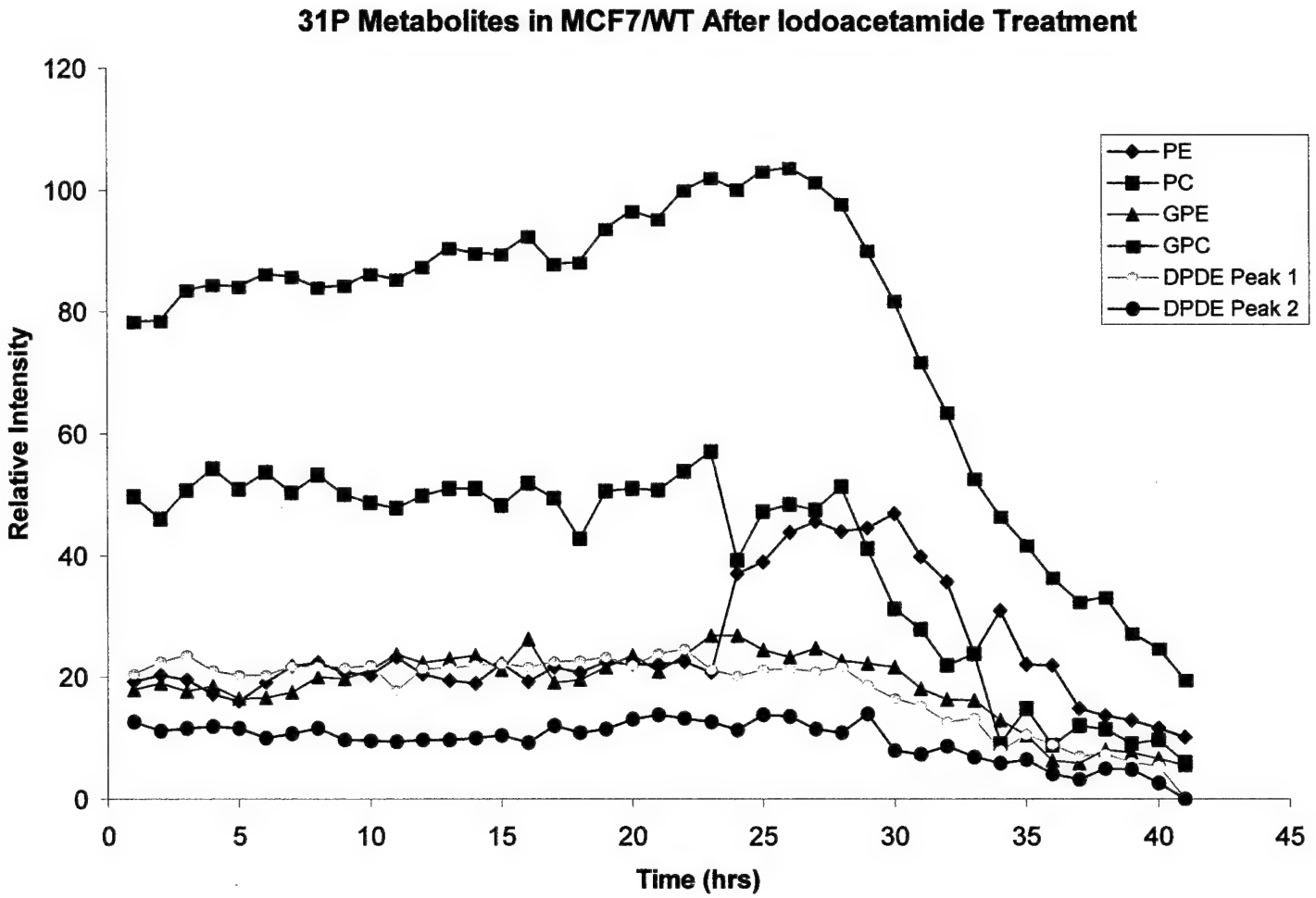

Figure 17. A drug sensitivity study. 10^8 MCF7/WT breast cancer cells embedded in the agarose gel perfused with growth medium were used. Forty-two ^{31}P NMR spectra were taken every hour. Each spectrum contains 1700 transients with 1 second repetition time. After 17 hours baseline study, 1mM iodoacetamide was added in the perfused medium. All the phosphorus metabolites concentrations are plotted as functions of time. Six metabolites are in this figure and the other five metabolites are in Figure 18. The concentration changes of the PE, PC, GPE, GPC and DPDE are plotted as function of time.

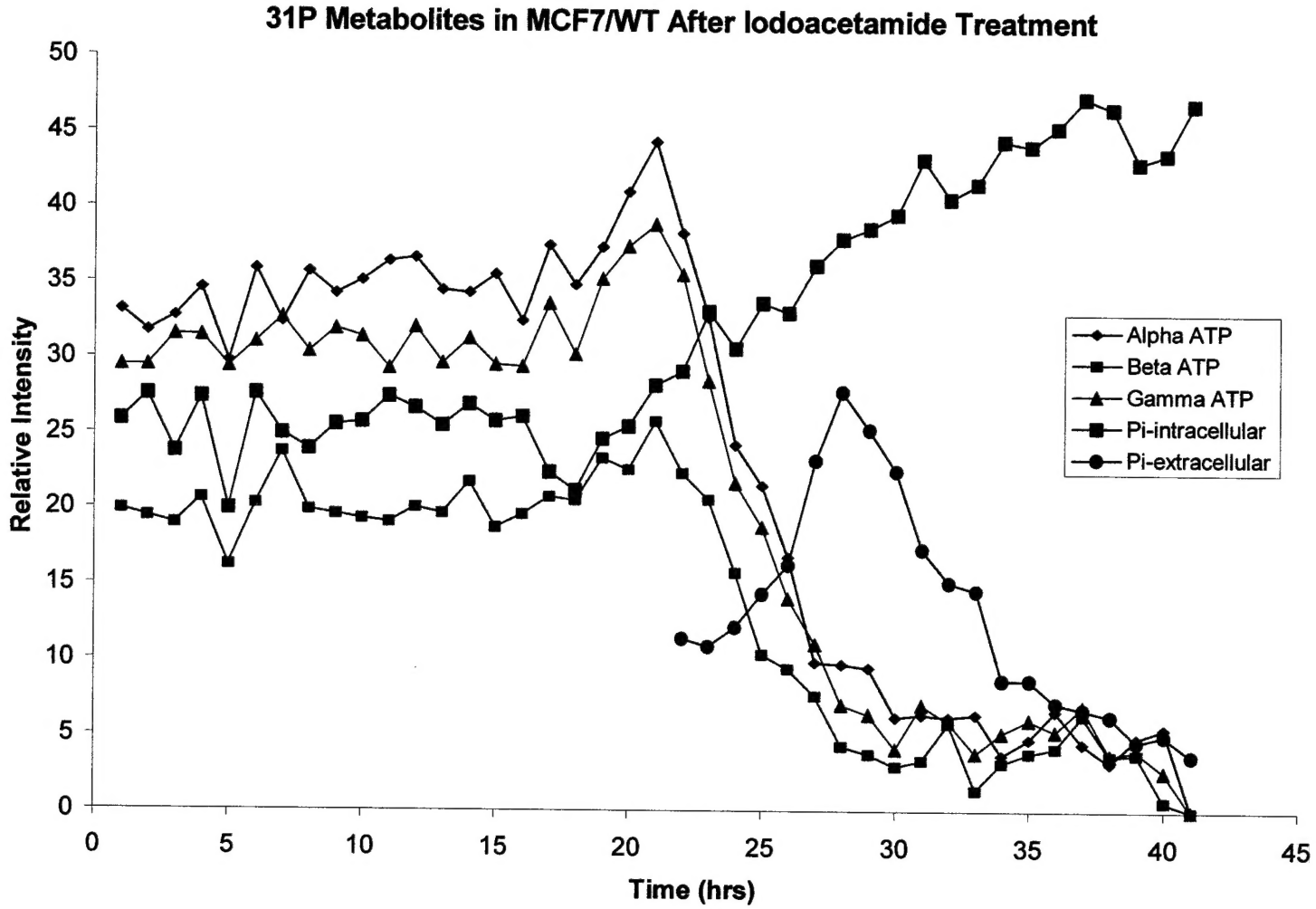

Figure 18. Concentrations of phosphorus metabolites before and after drug treatment. This figure contains the other five phosphorus metabolites: α-ATP, β-ATP, γ-ATP, intra- and extra- cellular Pi. The absolute concentrations are plotted as function of time.

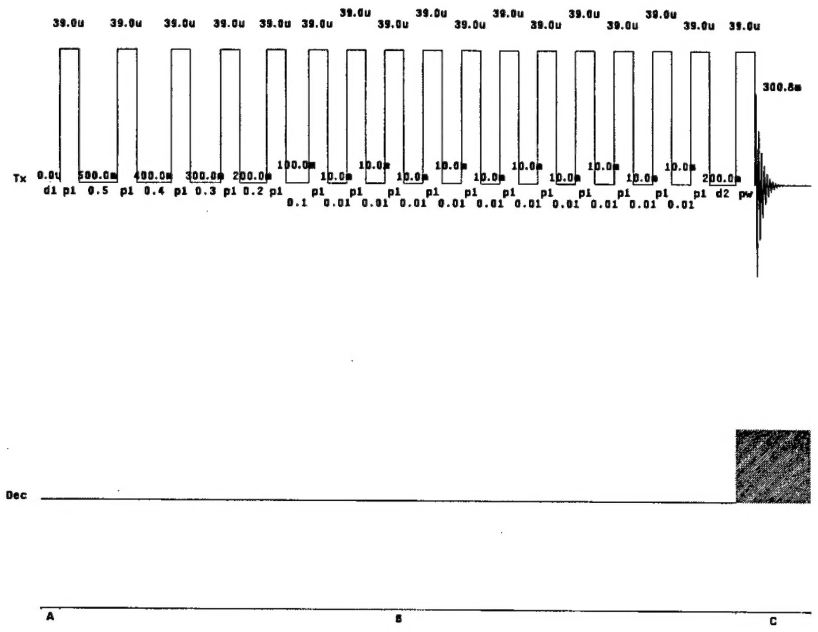

Name of Compound		Peak (ppm)	T1 (sec)	SD
Phosphoethanolamine(PE)		4.156	2.65	0.511
Phosphocholine (PC)		3.646	4.69	0.329
Inorganic Phosphate (intracellular)		2.631	5.36	1.031
Glycerolphosphoethanolamine(GPE)		0.892	>12	
Glycerolphosphocholine (GPC)		0.334	7.04	0.886
Phosphocreatine (PCr)		-2.633	3.04	1.30
Gamma ATP		-5.045	0.573	0.119
Alpha ATP		-10.132	0.606	0.084
Diphosphodiester Peak 1 (DPDE 1)		-10.844	1.45	0.112
Diphosphodiester Peak 2 (DPDE 1)		-12.557	1.60	0.271
Beta ATP		-18.612	0.383	0.055

Figure 19. T1 relaxation time measurement. The NMR T1 relaxation times of all the phosphorus metabolites of MCF7 breast cancer cells were measured with the improved NMR perfusion system. (A) A saturation recovery technique is used. A series of 16 RF pulses flips the magnetization to a horizontal plane first. It follows by a 90^0 RF pulse and data acquisition period. (B) A list of measured T1 relaxation times for each phosphorus metabolites. The T1 values vary from 0.38 seconds for β-ATP and longer than 12 seconds for GPE.

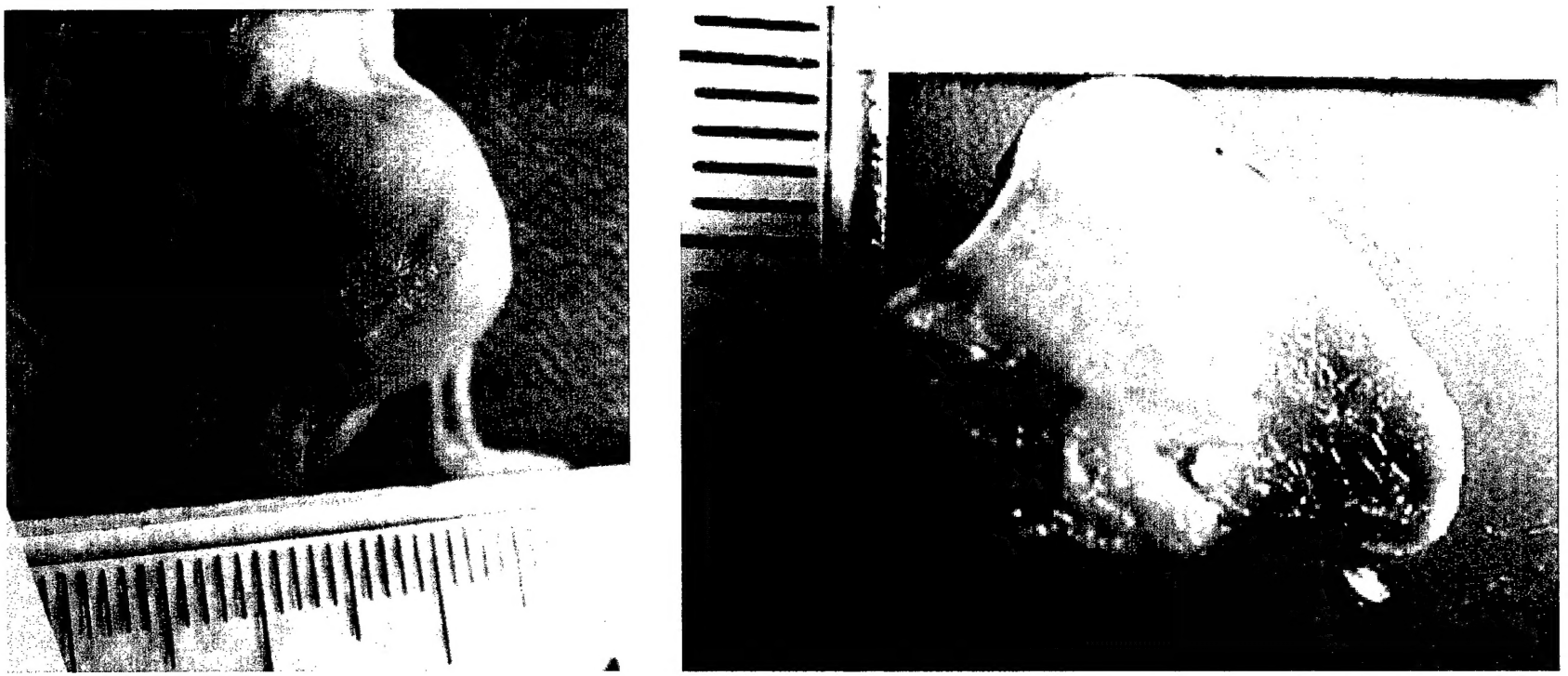

Figure 20. Solid tumor (MCF7 breast cancer) xenographs grown on nude mouse. The cutoff tumor specimen is shown on the right. The darker area on the both right and left side of the specimen indicates areas with more blood supply than the necrotic center. This image correlates well with the MRI images shown in Figure 21.

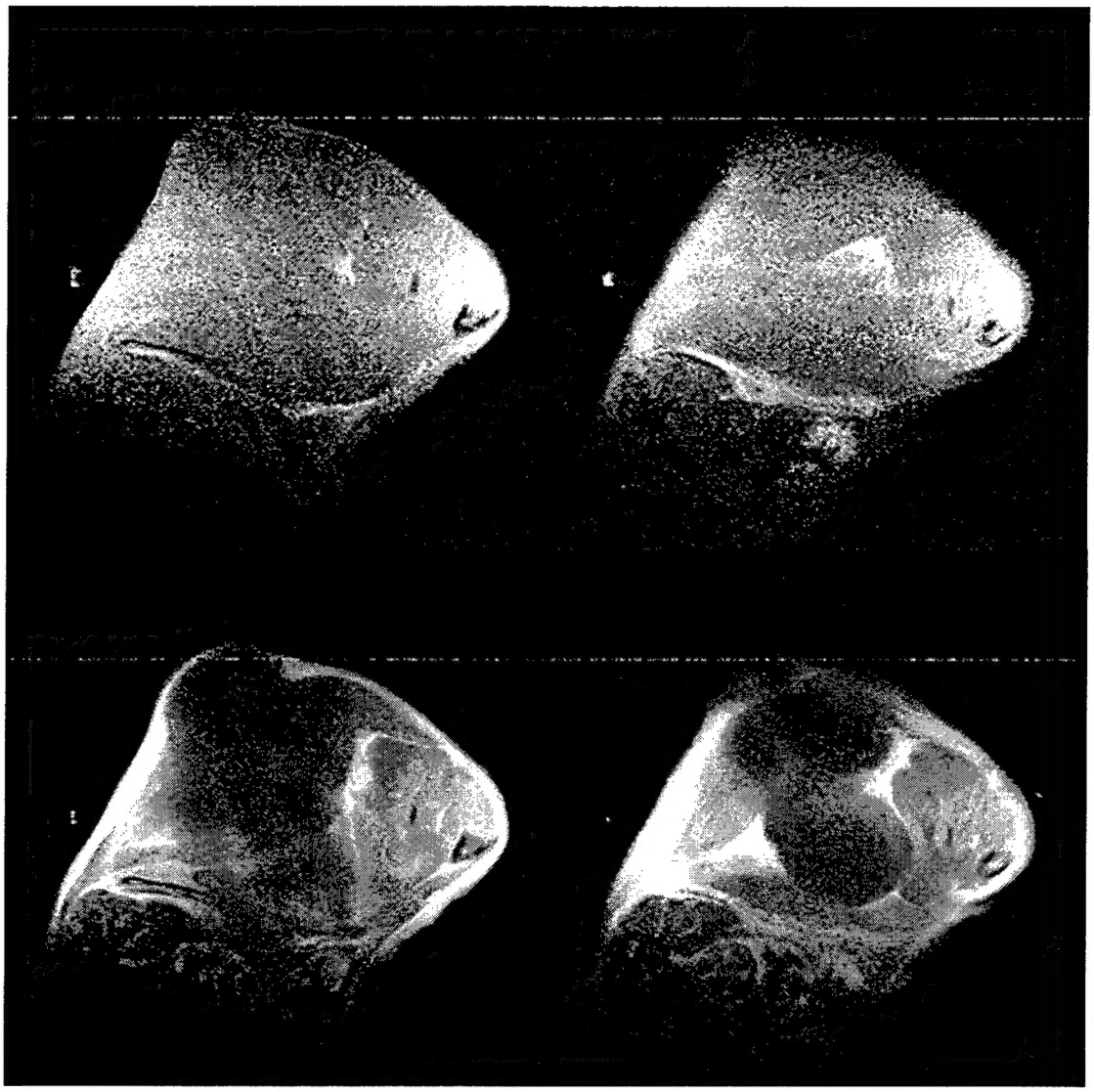

Figure 21. T1-weighted MRI images through the tumor. Two top images are before contrast agent injection. The bottom two images are after contrast agent injection. The enhanced areas indicate the presence of contrast agent.